

AN ABSTRACT OF THE THESIS OF

Robert W. Mittelstadt for the degree of Master of Science in Bioresource Engineering presented on June 9, 1995. Title: Characterizing Hydraulics and Water Distribution of Furrow Irrigation in Northeast Malheur County.

Abstract approved: Redacted for Privacy

Marshall J. English

Furrow irrigation is the dominant practice for irrigating row crops in the western Treasure Valley region near Ontario, Oregon. Though improvements have been made in management practices over the years, excessive runoff and deep percolation are still important problems contributing to surface water and groundwater degradation.

Field observations were made during two growing seasons to establish a data base from which the hydraulic surface irrigation model, SRFR¹, could be calibrated. SRFR is a numerical model, based on the principles of open channel hydraulics coupled with an empirical relationship characterizing furrow intake. SRFR is an analytical tool, with which the user supplies the physical parameters (such as furrow shape and furrow intake) and also the management

¹ SRFR, a computer program for simulating flow in surface irrigation, developed at the U.S. Water Conservation Laboratory in Phoenix, Arizona (Strelkoff, 1991).

variables (inflow rate and duration of inflow), and a simulation is conducted based on these conditions. Therefore, this model is a tool which provides insight into furrow irrigation processes. More specifically, SRFR can help answer such questions as which factors at the time of the irrigation are most important in determining irrigation performance. Once calibrated for a given set of conditions, various management strategies may be evaluated as to their relative effectiveness. These strategies may include, but are not limited to, cut-back irrigation, surge irrigation, alternating furrow irrigation, and laser-leveling of the field.

A broad data-base is necessary for model calibration and to develop an understanding of it's limitations. Measurements of furrow intake, stream advance times, inflow and outflow, hydraulic roughness and furrow shape were obtained from several sites and irrigation events. These sites represent several crops, field lengths, field slopes, and soil textures. Using these data, a model calibration procedure was developed which matched irrigation inflow and outflow volumes and stream advance times for a given irrigation event. The calibration procedure is used to help identify those model input parameters that best describe a given irrigation event. This thesis is to provide a broad understanding of furrow irrigation systems in northeast Malheur County, recommended hydraulic parameters for use with SRFR, and the practical limitations of such hydraulic irrigation models.

Irrigation performance is largely determined by the intake characteristics of the soil at the time of irrigation. Field conditions vary greatly depending on

the crop, soil moisture, number of irrigations, tractor traffic, field slope, furrow shape and field history. The grower has control over only two variables which determine irrigation performance: inflow rate and duration.

A difference in intake and irrigation performance was found to exist between non-wheel and wheel traffic furrows. These differences became less noticeable late in the season. Straw mulching greatly increases the furrow hydraulic roughness and therefore increases stream wetted perimeter and advance time. Vegetative interference from crops such as potato and sugar beets increase furrow hydraulic roughness late in the season. Initially, furrow shape depends on the crop and which cultivating implement is used. Furrow shape may evolve during the growing season depending on field slope, flow velocities, crop stand and the presence of crop residues and straw mulch.

**Characterizing Hydraulics and Water Distribution of
Furrow Irrigation in Northeast Malheur County**

by

Robert W. Mittelstadt

A THESIS

submitted to

Oregon State University

**in partial fulfillment of
the requirements for the
degree of**

Master of Science

**Completed June 9, 1995
Commencement June 1996**

Master of Science thesis of Robert W. Mittelstadt presented on June 9, 1995

APPROVED:

Redacted for Privacy

Major Professor, representing Bioresource Engineering

Redacted for Privacy

Chair, Department of Bioresource Engineering

Redacted for Privacy

Dean of Graduate School

I understand that my thesis will become part of the permanent collection of Oregon State University libraries. My signature below authorizes release of my thesis to any reader upon request.

Redacted for Privacy

Robert W. Mittelstadt, Author

ACKNOWLEDGMENT

This project would not have been possible without the efforts and contributions of many individuals and entities. First of all, many thanks to the USDA STEEP II program for funding this research effort in northeast Malheur County. In bringing this project to fruition, I gratefully acknowledge the support and friendship of my major professor, Prof. Marshall English, and Malheur Experiment Station superintendent, Prof. Clinton Shock. And to my committee members, Professors Pete Klingeman, John Selker and Tom Savage, I give thanks for their professional dedication and advice.

For invaluable technical assistance and cooperation I wish to thank Dr. Tom Trout of the USDA/ARS Research Unit at Kimberly, Idaho and Dr. Fedya Strelkoff of the USDA/ARS U.S. Water Conservation Laboratory in Phoenix, Arizona. Also providing technical assistance and cooperation were Herb Futter, formerly of the Malheur County Soil Water Conservation District (SWCD), Debbie Sherman and Ron Jones (Malheur Co. SWCD), Lynn Jensen with OSU Extension in Malheur County and Monty Saunders and Mike Barnum at the OSU Malheur Experiment Station.

Special thanks goes to the cooperating growers in northeast Malheur County: Bruce Cruickshank, Bill Duyn, Reid Saito, Keith Langley and the Max Barlow Family.

During my stay in Ontario, Oregon I enjoyed the hospitality of the staff and their families at the Malheur Experiment Station: Mary Jo Kee, Eric Feibert, Joey Ishida and Professor Chuck Stanger. I also wish to thank the many students employed at the Malheur Experiment Station whose company provided relief from the tedious boredom of field work: Nathan Tolman, Brad Turnbull, Joanna Zateiro, Cody Kankola and Mary Selfridge. I also wish to thank Joe Hobson and Randy Barnum for their friendliness.

I gratefully acknowledge the day-to-day assistance of my fellow graduate students Abdul Tunio and Syed Imran. Also, many thanks to graduate students Syed Raja, Russ Faux and Patrick Campagna for much valued companionship.

Lastly, I wish to thank my parents, Bill and Nancy Mittelstadt for their encouragement, and my kid sister, Amy, for her companionship.

TABLE OF CONTENTS

	<u>Page</u>
1. INTRODUCTION.....	1.
2. OBJECTIVES.....	5
3. THEORY.....	6
3.1 Infiltration into irrigated furrows.....	6
3.1.1 General equations.....	7
3.1.2 Intake relationships.....	8
3.1.3 SCS furrow intake curves.....	9
3.2 Open channel hydraulics.....	10
3.2.1 General equation.....	10
3.2.2 Zero-inertia assumption.....	11
3.2.3 Kinematic wave assumption.....	12
3.2.4 Manning equation and uniform flow.....	12
3.2.5 Volume balance model.....	14
4. LITERATURE REVIEW.....	16
4.1 Factors that affect furrow intake.....	16
4.2 Measuring and modeling furrow intake.....	18
4.3 Hydraulic modeling of surface irrigation.....	23
5. MATERIALS AND METHODS.....	28
5.1 Summary of irrigation sites.....	28
5.2 Furrow irrigation treatments.....	30
5.3 Furrow flow measurements.....	31
5.3.1 Calibration of flumes.....	32
5.3.2 Accuracy of measurements.....	33
5.3.3 Comparison with volumetric flow measurements...	33

TABLE OF CONTENTS (Continued)

	<u>Page</u>
5.4 Intake measurements.....	34
5.5 Soil moisture.....	36
5.5.1 Neutron probe.....	37
5.5.2 Gravimetric.....	39
5.5.3 Bulk density.....	39
5.6 Furrow channel geometry.....	40
5.7 Irrigation advance times.....	41
5.8 Manning's roughness and section factor.....	42
5.9 Irrigation scheduling.....	43
5.10 Irrigation efficiency and distribution uniformity.....	46
5.11 Model calibration.....	47
6. RESULTS.....	52
6.1 Furrow intake observations.....	52
6.1.1 Average intake curves.....	52
6.1.2 Long term intake rates.....	55
6.2 Manning's roughness and channel section factor.....	58
6.3 Furrow channel geometry.....	64
6.3.1 Furrow geometry summary.....	65
6.3.2 Selected furrow cross-sections.....	70
6.4 Calibration of the SRF model with field data.....	74
6.5 Seasonal variation in irrigation performance.....	95
7. SUMMARY.....	98

TABLE OF CONTENTS (Continued)

	<u>Page</u>
BIBLIOGRAPHY.....	102
APPENDICES.....	108
Appendix A Field descriptions.....	109
Appendix B Irrigation descriptions.....	113
Appendix C Variable notation.....	117
Appendix D Infiltration tests.....	119
Appendix E SRFR simulations output.....	122
Appendix F Field observations.....	123

LIST OF FIGURES

<u>Figure</u>		<u>Page</u>
5.1	The comparison of Powlus v-notch flume flow measurements with volumetric flow measurements made in the field. Data are from several irrigation events.....	34
6.1	Representative cumulative intake curves for bare non-wheel and wheel traffic furrows derived from inflow-outflow data. Data points from each intake test are also presented. These data are from the Barlow farm, Bel-Air Farms, and Fields B3 and B7 at the OSU Malheur Experiment Station.....	53
6.2	Long term intake rates for non-wheel and wheel traffic compacted furrows versus stream wetted perimeter. These data are from several farm sites throughout northeast Malheur County including the OSU Malheur Experiment Station.....	57
6.3	Normal depth as a function of Manning's roughness for several inflow rates given the field slope and furrow shape of Field B3 potatoes. Field slope is 0.030, side-slope $z = 2.00$ and channel bed-width $b = 14.5$ cm. OSU Malheur Experiment Station, Ontario, Oregon, 1994.....	61
6.4	Normal depth as a function of Manning's roughness for several inflow rates given the field slope and furrow shape of Field B7 spring wheat. Field slope is 0.0055, side-slope $z = 1.5$ and channel bed-width $b = 6.1$ cm. OSU Malheur Experiment Station, Ontario, Oregon, 1994.....	62
6.5	Wetted perimeter, P , versus furrow section factor, F , from several irrigation events during 1993 and 1994. Parameter F was calculated from the manning equation using estimates of Manning's n , inflow rate, Q_o , and field slope, S_o	64
6.6	Stream wetted perimeter, P , versus top width, T . Data are from several irrigation events observed during 1994 at the OSU Malheur Experiment Station and at several off-station sites.....	69

LIST OF FIGURES (Continued)

<u>Figure</u>		<u>Page</u>
6.7	Furrow cross-sections from MES Field B3 for a non-straw and straw mulched furrow after one irrigation. Field slope is approximately 3 percent and the soil is a Nyssa silt loam. OSU Malheur Experiment Station, Ontario, Oregon, 1994.....	71
6.8	Furrow cross-sections from MES Field B7 for a non-wheel traffic furrow prior to irrigation (May 11, 1993) and prior to harvest (August 27, 1993). Field slope is approximately 0.5% and the soil is a Greenleaf silt loam. OSU Malheur Experiment Station, Ontario, Oregon, 1994.....	72
6.9	Furrow cross-sections from the Cruickshank farm planted to corn. Cross-sections are from July 22 and July 25, 1993 prior to and after an irrigation following cultivation. The field slope is near 0.6% and the soil is an Owyhee silt loam.....	73
6.10	Wheel and non-wheel traffic furrow cross-sections from the Duyn sugar beet field, September 3, 1993. Cross-sections are from the tail of the field, at 274 m. Field slope averaged 0.9% and the soil is a Feltham loamy fine sand.....	74
6.11	Field observed and SRFR advance times of non-wheel and wheel traffic compacted furrows for the May 11, 1993 irrigation of Field B7 at the OSU Malheur Experiment Station, Ontario, Oregon, 1993.....	82
6.12	Distribution of infiltrated water on non-wheel traffic compacted furrow, May 11, 1993, Field B7, OSU Malheur Experiment Station, Ontario, Oregon.....	83
6.13	Distribution of infiltrated water on wheel traffic compacted furrow, May 11, 1993, Field B7, OSU Malheur Experiment Station, Ontario, Oregon.....	84
6.14	Field observed and SRFR simulation stream advance times for non-wheel and wheel traffic furrows from the April 12, 1994 irrigation of winter wheat at Bel-Air Farms.....	86

LIST OF FIGURES (Continued)

<u>Figure</u>	<u>Page</u>
6.15 Distribution of infiltrated water for a non-wheel traffic furrow, April 12, 1994, Bel-Air Farms.....	87
6.16 Distribution of infiltrated water on wheel traffic compacted furrow, April 12, 1994, Bel-Air Farms.....	88
6.17 Advance rates for the June 1, 1994 irrigation of potatoes on Field B3 at the OSU Malheur Experiment Station.....	89
6.18 Distribution of infiltrated water along a wheel traffic compacted, strawed furrow, June 1, 1994, Field B3, OSU Malheur Experiment Station.....	90
6.19 Distribution of infiltrated water along a wheel traffic compacted, non-strawed furrow, June 1, 1994, Field B3, OSU Malheur Experiment Station.....	91
6.20 Field observed and SRFR simulation stream advance times from the June 9, 1994 irrigation of potatoes planted on Field B3 at the OSU Malheur Experiment Station.....	92
6.21 Distribution of infiltrated water along a non-wheel traffic compacted, strawed furrow, June 9, 1994, Field B3, OSU Malheur Experiment Station.....	93
6.22 Distribution of infiltrated water along a non-wheel traffic compacted, non-strawed furrow, June 9, 1994, Field B3, OSU Malheur Experiment Station.....	94
6.23 Percent runoff for each irrigation of Field B7 during 1993 at the Malheur Experiment Station. Results are from both non-wheel traffic and wheel traffic furrows.....	96

LIST OF TABLES

<u>Table</u>		<u>Page</u>
4.1	Manning's n roughness from the literature.....	26
5.1	Field descriptions for each site where irrigation evaluations were conducted during 1993 and 1994.....	30
5.2	Location of furrow intake measurements.....	36
5.3	Neutron probe calibration coefficients.....	38
5.4	Irrigation management parameters for various crops.....	44
5.5	Soil series and available water capacities.....	45
6.1	Average intake coefficients to $Z=kt^a+bt+c$	54
6.2	Mean intake values and standard deviations.....	56
6.3	Manning's roughness for each irrigation event.....	59
6.4	Recommended Manning's n values.....	60
6.5	Wetted perimeter vs. section factor regression coefficients to $P=cF^p$ (units in cm).....	63
6.6	Furrow channel dimensions from profilometer results.....	67
6.7	Recommended furrow geometries.....	68
6.8	SRFR simulations and calibration fitting parameters.....	77
6.9	Inflow and runoff data from all observed irrigation events. Field data are compared with SRFR simulation results.....	79
6.10	Percent infiltration and runoff from all observed irrigation events. Field data are compared with SRFR simulation results.....	80
6.11	Field B7 runoff percentages from each irrigation, 1993.....	97

LIST OF TABLES (Continued)

<u>Table</u>		<u>Page</u>
A.1	Recirculating infiltrometer test results from MES Field B7 conducted during 1993. The field was planted to spring wheat. Soil type was a Greenleaf silt loam.....	119
A.2	Inflow-outflow infiltration test results from MES Field B7 conducted during 1994. The field was planted to winter wheat. Soil type was a Greenleaf silt loam.....	119
A.3	Inflow-outflow infiltration test results from MES Field B3 conducted during 1993. The field was planted to potato. Soil type was a Nyssa silt loam.....	120
A.4	Inflow-outflow infiltration test results from 1994 from three farm sites. Soils were all Nyssa silt loam.....	121
A.5	Summary of SRFR simulation results.....	122
A.6	Field observed irrigation performance.....	124

Characterizing Hydraulics and Water Distribution of Furrow Irrigation in Northeast Malheur County

1. INTRODUCTION

Northeastern Malheur County in Oregon contains approximately 350 square miles of productive irrigated farmland. This land is irrigated from several water sources: the Owyhee, Warm Springs, Buleah, and Bully Creek Reservoirs and the Owyhee, Malheur and Snake Rivers. Groundwater is also pumped for irrigation. Furrow irrigation is the dominant method of irrigating row crops. Major crops grown in this region are: potatoes, sugar beets, onions, grain, alfalfa, field corn, and various seed crops. The most prominent soil series are: Garbutt, Greenleaf, Nyssa, Owyhee, Powder and Virtue silt loams; Feltham loamy fine sands; and Kimberly, Sagehill and Turbyfill fine sandy loams.

The climate in this region is semi-arid with a mean annual precipitation of 232 mm (9.15 inches) based on a 10 year average (Barnum, et al. 1995). Cooler, wetter weather prevailed during much of 1993 when total precipitation was 338 mm (13.30 inches) or 45.4 percent above the 10 year average. Precipitation during 1994 was slightly above the 10 year average at 255 mm (10.05 inches). Mean annual free water surface evaporation (April through October) equals 1465 mm (57.73 inches) based on a 10 year average. Free water surface evaporation was 1206 mm (47.49 inches) and 1503 mm (59.19 inches)

in 1993 and 1994 respectively. Much of the region's drinking water comes from groundwater sources. Unfortunately, due to local high water table conditions, cultural practices in these areas can affect the groundwater quality of the shallow aquifer. The Oregon Department of Environmental Quality, in 1991, declared northeast Malheur County a "Groundwater Management Area" due to groundwater nitrate contamination, and has subsequently adopted a voluntary action plan. Though efforts have been made to increase efficiency of water and fertilizer use and to reduce runoff, research continues to be important for determining regional "best management practices" (BMP's).

With regards to energy, surface irrigation techniques are very efficient, requiring minimal pumping to deliver water to the crops in the field. But concerning crop water requirements, a larger volume of water is generally delivered to the field than is required by the crop. This disparity is due to the time required for flows to advance across the field and the additional irrigation time needed to meet water requirements at the tail end of the field. The result is over-watering of upper parts of the field and low water application efficiencies. Over-watering can leach nitrate-nitrogen from the crop root zone. The mobile nitrate anion readily moves with the soil-water and may consequently be leached past the crops roots and become unavailable. Loss of nitrate from the crop root zone poses a groundwater contamination risk, especially in areas where groundwater tables are shallow. Excessive runoff may likewise occur under poorly managed furrow irrigation practices. Runoff water can carry with it suspended and dissolved solids from the field along with

nutrients such as phosphorus. Although runoff generally results from furrow irrigation, carefully managed tail ditch systems can remove much of the suspended load before the water leaves the field.

James (1988) reports that surface irrigation systems (including furrow) typically have overall "on-farm" irrigation efficiencies of 50 to 70 percent. When properly managed, irrigation efficiencies can be as high as a well managed sprinkler system. It has been shown in studies (Anon., 1978) that overall efficiencies can approach that of sprinkler irrigation, or on the order of 70 percent.

Overall, the greatest difficulty in achieving high irrigation efficiencies while minimizing runoff and deep percolation is the different performance of each irrigation throughout the season. Crop stand, soil moisture, surface roughness, furrow geometry, and soil properties are all parameters that are not constant in space and time (Erie, 1962). Likewise, during a single irrigation there is a significant difference in stream advance rates between tractor wheel traffic compacted furrows and non-compacted furrows. The experience of the grower determines the irrigation management parameters; flow rate(s) and duration. In addition, effective management is made more difficult by variations in field slope, soil type, soil properties and field history.

For purposes of predicting and evaluating the performance of various furrow irrigation management practices, it is first necessary to adequately model the furrow irrigation process. A comprehensive hydraulic simulation model would be an analytical tool, able to account for variations in hydraulic

parameters such as slope, furrow intake and furrow shape. Initially, the model must be calibrated with field data from northeast Malheur County. A systematic method of model calibration will likewise be necessary.

The computer model, SRFR¹, was developed by the USDA Agricultural Research Service, U.S. Water Conservation Laboratory in Phoenix, Arizona (Strelkoff, 1990) for the purpose of surface irrigation analysis. This numerical model is based upon the principles of open channel hydraulics and is coupled with an empirical relationship which describes furrow intake. The zero-inertia or kinematic wave assumption may be employed by the model depending on the hydraulic conditions and user preference (see Section 3.2). The SRFR model is not meant for design purposes, but rather to provide insight into surface irrigation processes by allowing the user to alter irrigation parameters and to subsequently predict the resulting irrigation performance.

¹SRFR, a computer program for simulating flow in surface irrigation. Developed at the U.S. Water Conservation Laboratory in Phoenix, Arizona (Strelkoff, 1990).

2. OBJECTIVES

A principal objective of this thesis is to give the reader an understanding of furrow irrigation systems in northeast Malheur County. In addition, recommended hydraulic parameters for use with the SRFR model are presented based on field observations during 1993 and 1994. Lastly, the SRFR model is calibrated with field data from several irrigation events. These data help show the strengths and limitations of the SRFR model for use with furrow irrigation systems in northeast Malheur County. The specific objectives are outlined below.

1. Develop representative furrow intake curves for irrigated non-wheel and wheel traffic furrows to be used with SRFR.
2. Measure and discuss Manning's roughness values for bare soil furrows, furrows with vegetative interference and straw mulched furrows.
3. Measure and characterize furrow cross-sectional shapes for use with SRFR.
4. Calibrate the SRFR model for several irrigation events and sites using stream advance and furrow inflow and runoff data.
5. Show examples of variation in irrigation performance.

3. THEORY

This section describes the theoretical background for modeling furrow irrigation processes. The SRFR model is capable of determining a solution based upon the Saint-Venant equation (full hydrodynamic equation) for open channel flow, but to reduce computation time, the zero-inertia or kinematic wave assumptions have been shown to be applicable to furrow irrigation systems (Elliott and Walker, 1982b, Walker and Humpherys, 1983). The volume-balance model of Lewis and Milne (1938), solely based upon the continuity equation, has also been shown to be a useful modeling tool. Furrow intake is often modeled with an empirical relationship such as the Extended Kostiakov equation (Elliott and Walker, 1982a). Accordingly, the SRFR model allows the option of modeling intake with the Extended Kostiakov equation.

Numerous mathematical relationships are presented in this thesis, and so to aid the reader, a list of all notation is given in Appendix C.

3.1 Infiltration into irrigated furrows

Infiltration characteristics largely determine irrigation performance, therefore it is important to recall the theoretical background for soil-water dynamics.

3.1.1 General equations

The general equation for one-dimensional flow in porous media is Darcy's law, given as:

$$q = -K(h) \frac{dh}{ds} \quad (1)$$

where variable q is Darcy flux ($L \cdot T^{-1}$), h is soil-water potential (L), s is distance (L), and $K(h)$ is hydraulic conductivity ($L \cdot T^{-1}$) as a function of soil-water potential, h (Richards, 1931).

Initially, infiltration into irrigated furrows is relatively rapid as water infiltrates in a radial pattern from the saturated stream bed to drier conditions in the crop bed. The energy gradient that drives soil-water flow is the difference in soil-water tension plus the difference in gravitational potential over a unit distance. At a given location in the soil-water system, the total potential or head, h , is defined as,

$$h = h_t + h_g \quad (2)$$

where h_t is soil-water tension and h_g is gravitational potential with respect to some arbitrary datum (Richards, 1931).

3.1.2 Intake relationships

Physically describing infiltration into irrigated furrows is a mathematically complex task. Therefore, empirical relationships have been developed from field experience to characterize furrow intake. Examples of accepted relationships are the Kostiakov, Soil Conservation Service (SCS), and Extended Kostiakov equations.

The Extended Kostiakov equation is given as,

$$Z = k\tau^a + b\tau + c \quad (3)$$

where Z is cumulative intake in terms of volume of water per unit length of furrow (L^3L^{-1}) (Elliott and Walker, 1982a). Parameters k , a , b , and c are curve fitting parameters found through nonlinear regression. The b term approximates the "basic" or long term intake rate of the furrow. Parameters k , a , and c describe the transient portion of the curve. Opportunity time, τ , is the duration of time for which water is available for infiltration at a given point along the furrow. The Extended Kostiakov intake function is often used to describe intake in irrigated furrows because of its flexibility in fitting a wide range of measured intake curves, and also because the parameters have some physical basis (Elliott and Walker, 1982a).

The term *intake* is used in this thesis to describe the volume of water infiltrated per unit length of furrow having units of L^3L^{-1} . This is to be

distinguished from the term *infiltration* which is a general term describing the movement of surface water into the soil-water system.

3.1.3 SCS furrow intake curves

The Soil Conservation Service (SCS) has developed a system of intake curves (often referred to as "intake families") to represent the intake characteristics of different soils (SCS/USDA, 1984). Often, SCS furrow intake curves are the only information available for a given soil series. The SCS furrow intake curve has the form,

$$F = a\tau^b + 0.275 \quad (4)$$

where F is cumulative infiltration in terms of inches (L), and a and b are constants selected for the appropriate infiltration curve. Opportunity time, τ , is the time that water is available for infiltration at a given point along the furrow.

Within the SCS design algorithm, the nominal furrow wetted perimeter is given as,

$$P = 0.2686 \left(\frac{Qn}{\sqrt{S_o}} \right)^{0.4247} + 0.7462 \quad (5)$$

where P is in feet (L), Q is inflow rate in gpm (L^3T^{-1}), S is field slope ($L \cdot L^{-1}$) and n is Manning's roughness, a constant. Note that this is a nominal wetted

perimeter to be used with SCS furrow intake family curves and does not necessarily represent the actual wetted perimeter.

3.2 Open channel hydraulics

The governing equations of classical open channel hydraulics are used by SRFR to model flow in irrigated furrows.

3.2.1 General equations

The conservation of mass or continuity equation (Chow, 1959) is given as,

$$\frac{\partial A}{\partial t} + \frac{\partial Q}{\partial x} + \frac{\partial Z}{\partial t} = 0 \quad (6)$$

where A = the cross-sectional flow area (L^2); Q = the channel flowrate ($L^3 T^{-1}$); Z = cumulative infiltrated volume per unit length ($L^3 L^{-1}$) or intake; t = elapsed time (T) and x = distance (L). To completely describe flow in furrows, the continuity equation is combined with the dynamic equation for gradually varied unsteady (Chow, 1959).

$$\frac{1}{Ag} \frac{\partial Q}{\partial t} + \frac{2Q}{A^2 g} \frac{\partial Q}{\partial x} + (1 - Fr^2) \frac{\partial y}{\partial x} = (S_o - S_f) \quad (7)$$

Additional terms are: g , the gravitational constant ($L \cdot T^{-2}$); y is flow depth (L); S_o is channel bed slope ($L \cdot L^{-1}$); S_f is friction slope ($L \cdot L^{-1}$); and Fr is the Froude

number which is defined as,

$$Fr = \frac{Q^2 T}{A^3 g} \quad (8)$$

where T is stream top-width (L) (James, 1988). Froude numbers less than 1.0 indicate subcritical flow and Froude numbers greater than 1.0 show the flow to be supercritical. Subcritical flows are characterized by the normal depth, y_n , exceeding the critical depth, y_c , for a given channel.

3.2.2 Zero-inertia assumption

The zero-inertia approach simplifies the momentum equation by assuming that the rate of change in flow depth along the furrow equals the difference between bed slope and friction slope (James, 1988):

$$\frac{\partial y}{\partial x} = S_o - S_f \quad (9)$$

This assumption can be made when flow velocities are small, and the resulting Froude numbers are likewise small. The zero-inertia assumption has been tested against field data for furrows by Elliott and Walker (1982b) and Schwankl and Wallander (1988).

3.2.3 Kinematic wave assumption

The kinematic wave model assumes a friction slope, S_f , equal to the bed slope, S_o , and therefore uniform flow conditions and normal depth for the full length of the stream (James, 1988). This further simplifies the hydrodynamic equation to:

$$\frac{\partial y}{\partial x} = 0 \quad (10)$$

which allows the use of a uniform flow equation such as the Manning equation. The kinematic wave model has been tested for furrow irrigation by Walker and Humpherys (1983).

3.2.4 Manning equation and uniform flow

In the special case of uniform flow, the Manning equation may be applied:

$$Q = \frac{1}{n} \sqrt{S_o} A R^{2/3} \quad (11)$$

The R term is the hydraulic radius (L) which is equal to the flow area, A , divided by wetted perimeter, P . Manning's roughness, n ($T \cdot L^{-1/3}$) is an empirically determined value and is a function of several factors (Chow, 1959). The product of cross-sectional flow area and hydraulic radius raised to the two-thirds power, $AR^{2/3}$, is called the section factor, F . Under uniform flow conditions, the Manning

equation may be used to solve for the section factor.

$$F = \frac{Qn}{\sqrt{S_o}} = AR^{2/3} = \frac{A^{5/3}}{P^{2/3}} \quad (12)$$

Manning's roughness, n , sometimes referred to as a roughness coefficient, describes flow resistance under uniform flow conditions (Chow, 1959). There is no exact method of selecting an appropriate roughness value (Chow, 1959). Usually, the selection of a Manning's roughness coefficient requires field experience or the use of published data (see Section 4.3)

Factors affecting Manning's roughness n are given as: surface roughness, vegetation, channel irregularity, channel alignment, silting and scouring, obstructions, and channel size and shape (Chow, 1959). Because of these several primary factors, the value of n may be computed (Chow, 1959),

$$n = (n_0 + n_1 + n_2 + n_3 + n_4)m_5 \quad (13)$$

Additive roughness values are: n_0 for basic uniform channel, n_1 to account for surface irregularities, n_2 for variations in channel cross-section size and shape, n_3 for obstructions, and n_4 for vegetation. The coefficient, m_5 , is a correction factor for a meandering channel.

Channel roughness, to a great extent, determines the depth of flow of the irrigation stream. The greater the flow depth, the greater the wetted perimeter which in turn increases the surface area through which water may infiltrate.

Manning's n can be related to Chezy C by the following equation in the metric system (Chow, 1959):

$$C = \frac{1.49}{n} R^{\frac{2}{3}} \quad (14)$$

The Chezy C is an alternative method of characterizing the resistance to flow in the furrow by the SRFRR model.

3.2.5 Volume balance model

The volume balance model (Lewis and Milne, 1938, and Christiansen et al., 1966) is based solely on conservation of mass. A simplified form of the equation is given as:

$$Q_o t = \sigma_y A_o x + \sigma_z W Z_o x \quad (15)$$

where Q_o and t are mean furrow inflow rate and inflow duration respectively. Coefficients σ_y and σ_z are surface stream and infiltrated depth profile shape factors, respectively. The surface storage coefficient, σ_y , equals the mean cross-sectional flow area divided by the maximum flow area and is often assumed to be 0.77. Values of σ_y have been determined from field measurements of water surface profiles by Ley (1978) and Wilke and Smerdon (1965). Coefficient σ_z equals the mean infiltrated depth along the furrow divided by the maximum infiltrated depth and is determined by an iterative procedure. The furrow

spacing is W . The subscript y refers to stream depth and subscript z refers to infiltrated depth for the surface storage and infiltrated volumes respectively. Subscript o denotes values for the top of the field at the point of furrow inflow.

To model stream advance in the furrow, a power relationship is often used with the volume balance equation:

$$x=pt^r \quad (16)$$

Parameters p and r can be determined from an iterative procedure, simultaneously solving the volume balance equation for two or more points along the furrow. The value of exponent r is typically between 0 and 1. Nonlinear regression may also be used to determine p and r .

The volume balance method is popular for both irrigation analysis and design. This is due mainly to its ease of use and the relatively low number of computations required. In Section 4.4, the use of the volume-balance model for estimating furrow infiltration characteristics is discussed.

4. LITERATURE REVIEW

There is much relevant information from previous research. A review of the literature is given below.

4.1 Factors that affect furrow intake

A short discussion was given by Erie (1962) on factors affecting intake rates under gravity irrigated conditions. These factors include surface soil conditions, soil texture and structure, soil moisture content, crop stand and soil and water temperature.

Kemper et al. (1982) examined the effects of tractor wheel compaction on furrow intake and its importance to irrigation uniformity. Measured intake rates from 15 fields near Twin Falls, Idaho, showed wheel traffic compacted furrows to have a steady rate of $0.48 \text{ cm} \cdot \text{h}^{-1}$ compared with $0.89 \text{ cm} \cdot \text{h}^{-1}$ for non-compacted furrows (these intake rates are in terms of infiltrated volume per unit field width). In addition, Kemper et al. (1982) showed that the effect of tractor wheel compaction on intake rate depends upon soil moisture content at time of compaction, soil texture, the tractor mass and weight distribution.

Potential management tools to compensate for differences in intake opportunity time along the furrow were discussed by Kemper et al. (1982). One practice is straw mulching of the lower ends of the furrows to increase the wetted perimeter and intake and to decrease the flow velocity. The resulting

benefits are increased irrigation uniformity and a decrease in soil loss from the field (Shock et al., 1995). Another important practice is land grading for a shallower slope at the bottom of the field which increases flow depth, stream wetted perimeter and decreases flow velocity and erosivity.

The deposition of sediment to form a surface seal at the bottom of the furrow channel has important irrigation management implications. Observations were made by Brown et al. (1988) on the effect sediment adsorbed to the furrow wetted perimeter has on intake and erosion. Intake was found to be 33 to 50 percent lower in furrows carrying sediment enriched water than in furrows carrying clean water on a Portneuf silt loam with a 0.7 percent slope. Brown et al. also found that furrows carrying sediment laden water resisted erosion, allowing furrow shape to be preserved.

Irrigations following cultivation are typically characterized by the breakdown of soil clods in the furrow and the relocation and deposition of sediment along the furrow bottom as the stream advances, forming a surface seal (Trout, 1990). This consolidation of the soil in the furrow channel bottom results in more predictable irrigations later in the season if vegetative interference does not become important. Accordingly, Childs et al. (1993) found a high correlation of cumulative infiltration between the second, third and fourth irrigations following the cultivation of the furrows.

Several researchers (Fangmeier and Ramsey, 1978; Izadi and Wallender, 1985) have found that a positive relationship exists between furrow intake and wetted perimeter. Consequently, furrow intake must be related to hydraulic

factors such as flow rate, bed slope and roughness. To better understand these interactions, Trout (1992) investigated the steady state effects of flow velocity and wetted perimeter on furrow intake. It was stated that the effect of wetted perimeter on intake theoretically decreases with infiltrated volume as lateral flow in the soil profile becomes less important. Trout (1992) found no definitive relationship between steady intake rate and wetted perimeter. He concluded that intake increases with less than a proportional relationship with wetted perimeter when all other factors are held constant.

4.2 Measuring and modeling furrow intake

Several methods exist for measuring furrow intake. These include both direct methods and indirect methods.

Data obtained from an irrigation event can be used to directly establish an intake curve. The widely used inflow-outflow method requires the measurement of inflow and outflow for a furrow section at various times during the irrigation (Kincaid, 1986). Davis and Fry (1963), found good agreement between the volume balance equation (discussed in Section 3.2.5) and inflow-outflow results from field evaluations on a Panoche silty clay loam and a Yolo clay loam. They also noted that the inflow-outflow method requires flow measurements which partially obstruct the flow, often resulting in greater than normal flow depths near the flow measurement device.

The recirculating flow method has been in use since the early 1970's

(Nance and Lambert, 1970, Wallender and Bautista, 1983, and Blair and Trout, 1989). The recirculating infiltrometer test is based on the premise that it is important to mimic irrigation flow processes to best measure infiltration characteristics. This method uses a short length of furrow (on the order of 6 m (20 ft)) to which water is supplied from a constant head source. Water which reaches the downstream sump is pumped back to the top of the furrow segment. The change in storage in the supply reservoir over a given period represents cumulative infiltration as a function of time.

The ponded test method (also called stagnant blocked furrow test) uses a short furrow segment as in the recirculating flow method. Cumulative intake with respect to time is measured while a constant ponded depth is maintained. With the ponded test, no flow occurs along the furrow channel as is not the case during an actual irrigation. Fangmeier and Ramsey (1978) found ponded infiltration tests to underestimate intake when compared to volume-balance results. Bali and Wallender (1987) reported that ponded furrow test results are likely to be erratic on cracking soils.

On a smaller scale, a ponded test can be conducted using a by-pass infiltrometer during a surface irrigation (Shull, 1961). The infiltrometer is placed in the furrow and occupies one half of the furrow channel, allowing the irrigation advance stream to by-pass the infiltrometer. Simultaneously, the infiltrometer is filled with water to the same depth as the water outside the infiltrometer. As the irrigation progresses, water is added to the infiltrometer to maintain a ponded depth equivalent to that in the furrow. The amount of

water added with time is measured during the test to develop the intake curve. A similar test method, also conducted during an irrigation event, uses a "flow-through" infiltrometer which is situated in the furrow in a manner similar to the by-pass infiltrometer (Childs et al., 1993).

Several researchers have made use of the volume balance equation (described in Section 3.2.5) to derive intake curves (Davis and Fry, 1963, Elliott and Walker, 1982a, Smerdon et al., 1989, and Clemmens, 1991). Elliott and Walker (1982) used Christiansen's (1966) solution to the volume-balance equation as the means for establishing a "two-point" method for estimating infiltration functions from advance data.

With the "two-point" method, two advance data points are required. A power function is assumed to describe stream advance as a function of time.

$$x=pt^r \quad (17)$$

The volume-balance equation is then solved for these two stages of stream advance. Field experience suggests using the end of the field and the midpoint of the field for the two advance times, t_a and $t_{0.5a}$ (Burt et al., 1982, Elliott and Walker, 1982a). The power function exponent, r , is found by:

$$r = \frac{\ln 2}{\ln t_a - \ln t_{0.5a}} \quad (18)$$

where t_a is the total elapsed time for completion of advance. The volume balance is then solved for the two stages of stream advance. Terms V_a and $V_{0.5a}$ are

defined as follows:

$$V_a = \frac{Q_o t_a}{L} - 0.77A_o - \frac{bt_a}{(r+1)} \quad (19)$$

$$V_{0.5a} = \frac{2Q_o t_{0.5a}}{L} - 0.77A_o - \frac{bt_{0.5a}}{(r+1)} \quad (20)$$

Inflow rate is Q_o , the field length is L and A_o is the cross-sectional flow area at the top of the field. The long term intake rate is denoted by b .

The exponent term to the Extended Kostiakov equation, α , is found using:

$$\alpha = \frac{\ln V_a - \ln V_{0.5a}}{\ln(t_a) - \ln(t_{0.5a})} \quad (21)$$

The shape coefficient describing the subsurface distribution of infiltrated water, σ_z , is determined from α and r .

$$\sigma_z = \frac{\alpha + r(1-\alpha) + 1}{(1+\alpha)(1+r)} \quad (22)$$

Lastly, the Extended Kostiakov intake coefficient, k , is determined.

$$k = \frac{V_a}{\sigma_z t_a} \quad (23)$$

Elliott and Walker (1982a) found that inflow-outflow measurements best describe the long term or "basic" intake rate (approximated by b in the Extended Kostiakov equation) for use in the above "two-point" procedure. The distance

$$b = \frac{Q_o - Q_{ro}}{L} \quad (24)$$

between the inflow and outflow measurement points is L , which is often the length of the furrow. The long term or "basic" intake rate is defined to be the rate at which no greater than a 5 percent decrease in rate is measured over an hour. Steady conditions are generally achieved before the end of the irrigation.

Elliott et al. (1983b) and Elliott and Walker (1982a) found that the two term Extended Kostiakov equation better describes furrow intake than the original, single term Kostiakov equation, $Z = k\tau^a$. The Extended Kostiakov equation was chosen for several reasons. First, furrow irrigated soils do tend to exhibit a long term steady intake rate. Depending on soil texture and properties at the time of irrigation, long term intake rates are often reached before the irrigation is over. Secondly, the Extended Kostiakov equation allows additional flexibility for fitting intake data.

Theoretically, the intake rate of the furrow is partly a function of the interdependent parameters of furrow geometry, roughness, inflow rate, compaction and field slope. However, some question remains as to the relationship between flow velocity and furrow intake (Trout, 1992). Flow velocity becomes increasingly important with slope because of the corresponding increase in shear which encourages erosion. Additionally, Trout (1992) notes that shear is related to the square of the average flow velocity. A high roughness coefficient, as in the case of straw mulching, greatly diminishes flow velocity and increases furrow wetted perimeter.

Higher inflow rates can be set in non-wheel traffic furrows without

risking excessive runoff or erosion. Conversely, the lower intake rates of wheel traffic furrow do not warrant high inflow rates. Data presented by Tunio (1994) shows wheel traffic furrows to be more susceptible to erosion. He found that for field slopes ranging from 0.5% to 1.5%, the average sediment yield from non-wheel traffic compacted furrows was about 73% of the sediment yield in adjacent wheel traffic furrows.

4.3 Hydraulic modeling of surface irrigation

In recent years, models of surface irrigation hydraulics have been developed to more fully model the complexities of the irrigation process, and to better predict irrigation performance. Most of these simulation models have been validated with field data. That is, they have been shown to adequately model furrow irrigation advance and in some cases, stream recession also.

A hydraulic model based on the kinematic-wave assumption for open channel flow and coupled with the Extended Kostiakov equation was developed by Walker and Humpherys (1983) to model both continuous and surge irrigation of furrows. This model was calibrated with continuous irrigation field data from three Colorado sites, a Utah site and an Idaho site. This model was also calibrated with field data from the Utah and Idaho sites for surge irrigation.

Based on the zero-inertia assumption for border irrigation, described originally by Strelkoff and Katapodes (1977) and presented in Section 3.2.2, Elliott and Walker (1982b) developed a zero-inertia computer model for

conventional furrow irrigation. This zero-inertia model was later adapted to surge flow irrigation (Oweis and Walker, 1990). The Oweis and Walker model was calibrated with surge flow data from Utah and Idaho. In a separate effort, a zero-inertia model was developed by Schwankl and Wallender (1988) in California which allowed for intake as a function of wetted perimeter. To accommodate this assumption, a uniform flux across the wetted perimeter boundary was assumed.

Because wetted perimeter varies with flow depth, Strelkoff (1984) addressed the problem of modeling the effect of depth of flow on intake in computer simulations. Furrow intake must be normalized by stream wetted perimeter, P , if the effect of depth on stream wetted perimeter is to be included in the computer model. Normalized cumulative intake is denoted by the variable Z_n where units are in terms of length (L) and Z is cumulative intake in terms of volume per unit length (L^3L^{-1}). The relationship between Z_n and Z is defined in equation 25.

$$Z_n = \frac{Z}{P} \quad (25)$$

Furrow intake may be normalized by either stream top width, T , or by wetted perimeter, P , based on local depth. Strelkoff (1984) found that slightly better simulations resulted from normalizing with stream wetted perimeter, P .

In a later contribution, Strelkoff (1992), proposed a modification of the SCS intake family curves (equation 4) to allow for the use of these curves in

computer simulations where intake is made a function of wetted perimeter. His modification employs the ratio of the SCS nominal wetted perimeter, P , from equation 5, and the theoretical wetted perimeter, P_n , calculated from the normal depth for the given inflow rate. It was proposed that the SCS intake family constants, α and 0.275, be multiplied by the ratio P/P_n and then be used directly in the Extended Kostiakov equation (equation 3).

The roughness coefficient is usually represented by the Manning's n . Little research has been conducted to directly determine roughness coefficients for irrigated furrows under various conditions. Field determinations of Manning's n roughness have been made by Lindeman and Stegman (1971), Fangmeier and Ramsey (1976) and Trout (1992). Table 4.1 summarizes the findings from the literature for several western states. Some of the Manning's n roughness values reported are "design" values rather than field measured.

Table 4.1 Manning's n roughness from the literature

Location	n	Inflow ($l\ s^{-1}$)	Slope ($m\ m^{-1}$)	Crop
Arizona ¹	0.02	1.7	0.0010	bare
North Dakota ²	0.02	1.4	0.0051	potatoes
	0.02	2.4		
	0.02	1.2		
	0.03	1.3		
	0.03	1.7		
	0.04	0.9		
	0.06	0.7		
Utah ³	0.04*	2.00	0.0080	
Idaho ³	0.04*	0.80	0.0104	
	0.04*	1.50		
California ^{4&5}	0.065	1.00	0.0023	grain sorghum
	0.07	1.00	0.002	barley
Colorado ³	0.02*	1.14	0.0044	corn
	0.02*	3.49	0.0025	corn
	0.02*	0.92	0.0095	corn
	0.03*	1.00	0.0057	

*Asterisk indicates design values.

¹ Fangmeier and Ramsey, 1976.

² Linderman and Stegman, 1971.

³ Walker and Humpherys, 1983.

⁴ Schwankl and Wallender, 1988.

⁵ Tarboton and Wallender, 1989.

In the course of developing surface irrigation models, methods of model calibration have been developed to match simulation data with field data.

Bautista and Wallender (1993a) investigated an objective function used for the purpose of calibrating furrow intake parameters from advance data. In this case a finite-difference hydrodynamic model was used to predict stream advance times. A convergence procedure was then used to minimize the squared differences between predicted and observed advance data by varying the intake coefficients to the Extended Kostiakov equation. The first calibration method was based on minimizing the squared differences between predicted and observed advance times. The second method minimized the squared differences between the predicted and observed advance velocities. Advance velocities were calculated from advance data and not directly measured.

It was found that with large data sets, the identification procedure became susceptible to noisy field measurements when attempting convergence for three of the Extended Kostiakov parameters, k , a and b . The c parameter was assumed to be zero. Bautista and Wallender (1993a) found that the identification procedure worked well when fitting two of the three parameters to the Extended Kostiakov equation and assuming the value of the third parameter. It was noted that for practical reasons, the assumed parameter should be the term b , which approximates the long term intake rate, because this value can be readily measured in the field.

5. MATERIALS AND METHODS

The data presented within this thesis represent a wide variety of experimental observations and procedures. A discussion of irrigation sites and furrow treatments is followed by a discussion of methods used to measure furrow flow rates, soil moisture, furrow channel shape (geometry) and stream advance times. Also discussed are the methods used to determine Manning's roughness, irrigation depth required (irrigation scheduling), irrigation efficiency and SRFR model calibration.

The field procedures described in this chapter are the means by which irrigation performance is determined. In addition, these data are used to calibrate the SRFR simulation model for a given field and irrigation event. That is, by adjusting model input parameters, the simulation will, ideally, model results observed in the field. Moreover, it is anticipated that the relative importance of such factors as furrow intake, hydraulic roughness and furrow shape will properly be modeled for a given irrigation event.

5.1 Summary of irrigation sites

A total of nine irrigation evaluations were conducted at the Malheur Experiment Station during the 1993 and 1994 growing seasons. Five irrigations during the 1993 season were evaluated for a laser-leveled, 2.4 ha (6.0 acre) field planted to spring wheat. In addition, four irrigations were evaluated during

1994 on a 0.57 ha (1.4 acre) field planted to potatoes. Soil moisture for these fields at the experiment station was monitored using a neutron probe soil moisture gauge. Soils encountered at the experimental station were Greenleaf and Nyssa silt loams.

Four additional irrigation evaluations were conducted off-station at four different sites. The soil series represented at most of these sites were Nyssa and Owyhee silt loams although a Feltham series loamy fine sand was encountered at the Duyn farm. Table 5.1 summarizes the dates and field descriptions of each irrigation. Appendices A and B describe these fields in greater detail.

Table 5.1 Field descriptions for each site where irrigation evaluations were conducted during 1993 and 1994.

Name	Length m	Slope m m ⁻¹	Soil	Crop
MES B7 *	195	0.0055	silt loam	spring wheat
MES B7 *	195	0.0055	silt loam	winter wheat
MES B3 *	76	0.0300	silt loam	potatoes
Cruickshank	390	0.006	silt loam	corn
KLG Farms	165	0.0056	silt loam	dry beans
Duyn	274	0.0088	loamy fine sand	sugar beets
Bel-Air Farms	366	0.0103	silt loam	winter wheat
Barlow	378	NA	silt loam	winter wheat
Barlow	378	NA	silt loam	sugar beets

* OSU Malheur Experiment Station.

5.2 Furrow irrigation treatments

There are several important irrigation management treatments pertinent to this research. These include wheel traffic compaction of furrows, straw mulching and the number of irrigations following cultivation.

For most irrigation evaluations, both uncompacted and wheel traffic compacted furrows were under observation. Furrow compaction by wheel traffic greatly diminishes its ability to absorb water, resulting in a significant difference in irrigation performance between uncompacted and wheel traffic compacted furrows.

There are differences in irrigation performance between early season and late season irrigations. Early season irrigations are usually in freshly cultivated furrows. Furrows may be cultivated again in the spring and early summer prior to layby (when tractor traffic is no longer possible). Late in the season, furrows that have been subject to several irrigations often have an altered furrow shape, reduced permeability, but may also have vegetative obstructions.

In 1994, MES Field B3 consisted of 12 straw mulched experimental plots and 12 non-straw mulched plots. Straw was applied to these furrows at a rate of 1020 kg · ha⁻¹ (910 lb ac⁻¹). The purpose of research conducted on this field was to quantify differences in runoff water quantity and quality between straw mulched and non-straw mulched furrows. Both wheel traffic and non-wheel traffic furrows were irrigated during the season.

5.3 Furrow flow measurements

For most furrow inflow and outflow measurements, trapezoidal fiberglass flumes were used (Powlus v-notch flume, Honkers Supreme, Twin Falls, Idaho). This flume was originally developed by Robinson and Chamberlain (1960) at

Washington State College. Occasionally, volumetric flow measurements were made when not enough flumes were available for a particular experiment or to verify flume flow readings. For midfield flow measurements, v-notch flumes were used because of the ease of installation and minimal destruction to the furrow although some obstruction of the natural furrow flow regime is unavoidable. A hand-held torpedo level was used to check the level of the flume in the field, both longitudinally and laterally.

5.3.1 Calibration of flumes

Calibration of the flume is required due to the unique head-discharge relationships of different flow measurement devices. Trout (unpublished) with the USDA Agricultural Research Service at Kimberly, Idaho, discusses the installation and use of the v-notch flume. The following calibration equation (equation 26) was derived by Trout (unpublished) for scale readings, h , in

$$Q=0.0612(h-0.15)^{2.63} \quad (26)$$

$$Q=0.00386(h-0.15)^{2.63} \quad (27)$$

centimeters and flows, Q , in gallons per minute (gpm). For flows in liters per second, equation 27 is used.

5.3.2 Accuracy of measurements

The accuracy of flow measurements with v-notch flumes depends upon having a correct installation and upon the care taken in reading the upstream head, h . Most importantly, the flume must be level. Trout (unpublished), shows that the flow measurement error, ϵ_Q , is 2.63 times the relative gauge reading error, ϵ_h/h . That is:

$$\epsilon_Q = \frac{\epsilon_h}{h} 2.63 \quad (28)$$

where ϵ_h is measurement error in centimeters. Trout and Mackey (1988), in an analysis of furrow flow measurement accuracy, show that scale reading standard deviations are in the range of 1 to 2 mm. Furthermore, accuracies of h readings less than 2 mm are difficult to achieve in the field. At a flowrate of 0.63 l s^{-1} (10 gpm), a gauge reading of 7.1 cm, and a reading error of 2 mm, the resulting flow measurement error is $\pm 7.4\%$ or $\pm 0.047 \text{ l s}^{-1}$ (0.74 gpm).

5.3.3 Comparison with volumetric flow measurements

To verify the use of flumes with the given calibration equation, volumetric flow measurements were made in the field and compared with flume readings. Volumetric flow measurements were made at several sites under a wide range of flow conditions (0.05 to 0.7 l s^{-1} or 0.8 to 11.1 gpm). These

measurements were typically made using a 3.1 liter container and a stop-watch. Volumetric flow measurements compared closely with flume flow readings with an r^2 of 0.99 (Figure 5.1).

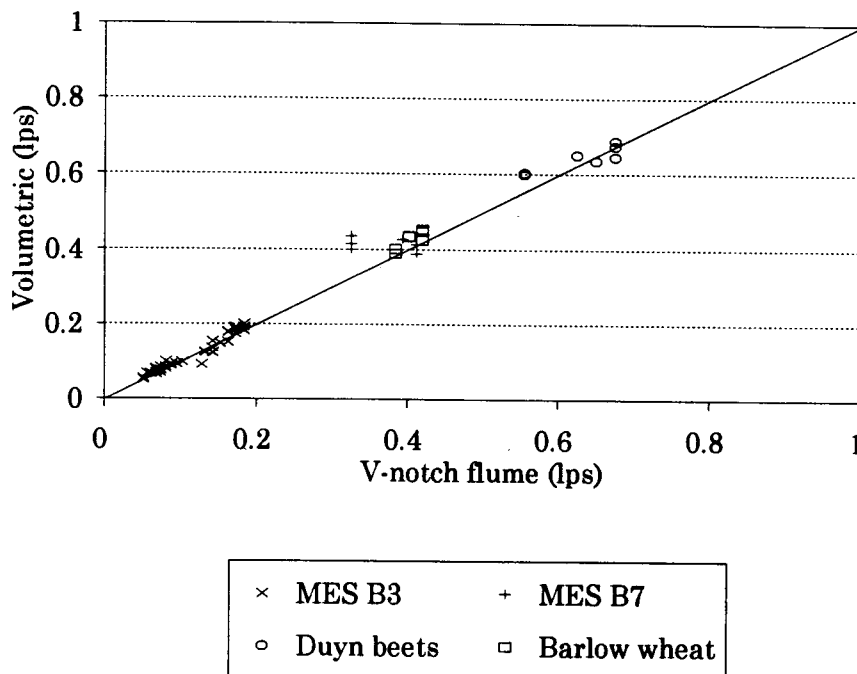


Figure 5.1 The comparison of Powlus v-notch flume flow measurements with volumetric flow measurements made in the field. Data are from several irrigation events.

5.4 Intake measurements

To obtain time series data of infiltration into irrigated furrows, direct intake tests were conducted using a recirculating infiltrometer (Blair and Trout, 1989) and the furrow inflow-outflow method (Kincaid, 1986). These tests help show the effect of furrow condition and treatment on furrow intake and the data

will be used to develop intake curves for use with the SRFR model.

A total of six recirculating infiltrometer tests were conducted, five of them on Field B7 at the Malheur Experiment Station on a Greenleaf silt loam, and one off-station on a Turbyfill sandy loam near the Snake River. Numerous pieces of equipment were required to perform these tests most of which were unavailable commercially in ready-to-use form. Observations were made according to instructions provided by Blair and Trout (1983). The recirculating infiltrometer used for these tests was provided by Dr. Tom Trout at the USDA-ARS facility in Kimberly, Idaho. The tests were generally conducted on a section of furrow 6.1 meters (20 feet) in length. The duration of the tests ranged from 6 to 8 hours with an average furrow inflow rate of 0.30 l s^{-1} (4.75 gpm).

Intake data were also obtained in the field using the inflow-outflow method with an irrigation (Section 4.2). Powlus v-notch flumes were used to measure in-furrow flow rates. The location of the outflow (or downstream) flume along the furrow section depends upon furrow conditions at the time of irrigation. For example, for first irrigations of non-wheel traffic furrows, the spacing chosen ranged from 45 to 90 m (150 to 300 ft). For wheel traffic compacted furrows, which have lower permeabilities, longer spacings of 75 to 120 m (250 to 400 ft) were used. Initially, flow rates were measured at 15 minute intervals after the advancing stream reached the outflow flume. After 2 hours, flowrates were measured hourly.

Table 5.2 Location of furrow intake measurements

Name	Soil	Crop	Method	No. obs.
MES B7*	silt loam	spring wheat	recirc.	5
MES B7*	silt loam	winter wheat	in-out	5
MES B3*	silt loam	potatoes	in-out	14
Duyn farm	fine sandy loam	no crop	recirc	1
Barlow farm	silt loam	sugar beets	in-out	2
Barlow farm	silt loam	winter wheat	in-out	2
Bel-Air Farms	silt loam	winter wheat	in-out	2

* OSU Malheur Experiment Station.

5.5 Soil moisture

To assess the soil moisture conditions prior to each irrigation and to help determine the distribution of water following the irrigation, a neutron probe soil moisture gauge was used at the Malheur Experiment Station. A $\frac{3}{4}$ inch (1.9 cm) soil probe was used to obtain gravimetric samples at off-station sites.

5.5.1 Neutron probe

Neutron probe access tubes were used to monitor soil moisture in two fields during the 1993 and 1994 growing seasons. Schedule 40 PVC tubing, 5.1 cm (2 inch) outside diameter and 1.8 m (6 ft) in length was used for neutron probe access tubes in Malheur Experiment Station Fields B3 and B7. A total of 28 tubes were placed in Field B7. For both non-wheel and wheel traffic furrows, two access tubes per furrow were placed every 30.5 m (100 ft) (one per crop bed on opposite sides of the furrow), for a total of 14 tubes per furrow.

In Field B3, a total of 16 neutron probe access tubes were used, four per furrow with four furrows under observation. These tubes were placed in the center of the crop bed at 9.1, 27.4, 45.7 and 64.0 meter (30, 90, 150 and 210 foot) distances down the furrow.

Neutron probe readings were taken immediately before and approximately 48 hours after each irrigation at 30 cm (1 foot) depth increments to a depth of 180 cm (6 feet). For the field trials of 1994, a standard count was taken before each session. The duration of each count was 32 seconds with the Campbell Pacific Nuclear probe and 15 seconds with a Troxler probe.

Calibration equations are needed for relating volumetric water content to neutron probe count. Also, these soil moisture gauges must typically be calibrated separately for readings near the surface due to the decreased sampling volume. The general equation is of the following linear form where volumetric water content, θ_v , is directly correlated with neutron probe counts:

$$\theta_v = K_1 \text{count} + K_2 \quad (29)$$

Coefficient K_1 is the slope of the neutron count versus volumetric soil moisture relationship and K_2 is the offset when *count* equals zero. Table 5.3 gives the calibration coefficients for both the Campbell Pacific Nuclear (CPN) and Troxler gauges used in this study.

Table 5.3 Neutron probe calibration coefficients

Unit	Depth cm	ft	K_1 cm cm ⁻¹ count ⁻¹	K_2 cm cm ⁻¹
CPN	0-30	1	0.000054	-0.083
CPN	30-180	2-6	0.000066	-0.22
Troxler	0-30	1	0.00077	0.090
Troxler	30-180	2-6	0.00094	-0.14

The coefficient of determination (r^2) values for these calibration equations were 0.92, 0.74, 0.92 and 0.86 respectively. These best-fit relationships were found through linear regression using data from 1992 and 1993. In 1993, 35 gravimetric samples were obtained from the soil profile, seven samples at every 31 cm depth (12 in) beginning at 31 cm. Three neutron probe counts were obtained for every single gravimetric sample. To derive the neutron probe

calibration equations for use near the soil surface, data from a 1992 study were obtained. These data consisted of 15 gravimetric and neutron probe samples taken at a depth of 15 centimeters (0.5 ft). For each gravimetric sample, five CPN neutron probe counts were obtained and the average was calculated for use in the regression analysis.

5.5.2 Gravimetric

Gravimetric soil samples were taken at off-station sites (Table 5.1) before and after irrigations. A 1.9 cm (0.75 inch) diameter soil probe with a sliding hammer was used to obtain samples from 30, 61 and 91 centimeter depths (1, 2 and 3 ft). The entire 30 cm (12 inches) at each depth was sampled. The soil sample was immediately placed in air-tight cans, weighed, dried, and weighed again. Samples were dried at 105 C for 24 hours prior to obtaining dry weight. Soil bulk density values were used to calculate volumetric soil moisture content from soil gravimetric data.

5.5.3 Bulk density

Bulk density samples were obtained using a 2 inch diameter cylindrical soil core sampler with a hammer driver. Sample volume was 97 cm³ (5.9 in³). Samples were taken from the furrow bottom, the crop bed and 30 cm (12 inches) below the bottom of the furrow. Bulk density samples were not obtained using

the soil core sampler for depths greater than 61 cm (24 in). For depths greater than 61 cm, where samples were not obtained, bulk density was assumed to be 1.4 g cc^{-1} based on previous research work at the experiment station.

5.6 Furrow channel geometry

For measuring the cross-sectional geometry of furrows under observation, a profilometer or "rill-meter" was used, provided by Dr. Tom Trout of the ARS facility in Kimberly, Idaho. This device consisted of multiple fiberglass rods held at two centimeter spacings on-center. These rods were held in place by a spring tensioned clamp immediately in front of a one centimeter spaced grid. The vertical scale increments were at two tenths of one centimeter.

The profilometer was placed above the furrow and the rods gently released to drop to the bottom of the furrow. The furrow shape was then profiled on the grid by the tops of the fiberglass rods. The date and location was identified with each furrow cross-section and a photograph of the grid was taken for a permanent record of the furrow geometry. Later, a line was drawn by hand through each data points for each side-slope and through the data points at the bottom of the furrow channel. The intersection of these lines determined the bottom width, b , and the average furrow side-slope, z , was also calculated.

In addition to profilometer observations of furrow shape, measurements of stream wetted perimeter, flow depth and stream top width were also obtained

using a flexible measuring tape. This tape had a scale in both inches and centimeters. Wetted perimeter measurements were made by fitting the tape to the bottom of the furrow by hand while holding the zero mark of the tape at one of the stream edges. Flow top width measurements were made by holding the tape tightly over the width of the stream. Flow depth measurements were made by lowering the end of the tape into the deepest part of the stream. Flow depth measurements were more subjective, with results relying somewhat on technique due to the shifting characteristics of the channel bottom, the flowing of water and the meniscus formed between the water surface and the tape. Also, the materials making up the channel bed were easily displaced, sometimes making the bottom of the channel difficult to discern. Measurements of wetted perimeter, top-width and flow depth were obtained at four locations along a furrow section (the same section as the inflow-outflow intake test). These measurements were repeated 4 to 6 times during the irrigation.

5.7 Irrigation advance times

The advance times of irrigation streams were monitored for each irrigation event. Stations were typically established at 30.5 m (100 ft) increments with the first station at 0+00 m, being the furrow inlet at the top of the field. The time at which the stream reached each station was recorded by hand using a digital stop-watch which was started at the beginning of the irrigation. Stream recession times were not recorded.

5.8 Manning's roughness and section factor

The Manning equation was used with measured stream flow depths, after steady conditions were achieved, to estimate Manning's roughness coefficient, n . Measurements taken to calculate Manning's n were: mean flowrate for the reach (Q_{avg}), mean bed slope (S_o), and flow depth (y). A profilometer (see Section 5.5) was used in the field to measure furrow shape.

An iterative procedure was used to find the roughness n at which the measured flow depth, y , equals the theoretical normal flow depth, y_n , for the given conditions. Usually, 4 or 5 iterations were required.

In summary, the procedure to determine Manning's n is as follows:

1. Measure steady rate Q_o , Q_{ro} for the reach and calculate the average, Q_{avg} . The reach is defined as the longitudinal section of furrow over which measurements are made.
2. Measure average field slope, S_o .
3. Measure channel shape with the profilometer. For a trapezoidal geometry, side-slope, z , and channel bottom width, b , are required.
4. Measure flow depths within the reach late in the irrigation and calculate the average depth, y .
5. Calculate the theoretical value for normal depth, y_n , for the given Q_{avg} , S_o , z and b and an assumed value for Manning's n .
6. Adjust Manning's n until y equals y_n .

5.9 Irrigation scheduling

To determine depth of irrigation required, Z_{req} , the mean antecedent soil moisture was measured prior to an irrigation. This value was subtracted from the field capacity, fc , to yield soil water depletion in cm cm^{-1} (in in^{-1}). Based on the concept of a soil-water budget for the crop root zone, the maximum available water in the root zone (AW) and the readily available water (RAW) are defined as:

$$AW = D_{rz}(fc - pwp) \quad (30)$$

$$RAW = D_{rz}(fc - \theta_c) \quad (31)$$

The effective depth of the root zone, D_{rz} , is determined from either field measurements or from compiled representative values for various crops (Table 5.4). Field capacity, fc , and permanent wilting point, pwp , are irrigation management parameters, and can be estimated from the literature or from field experience. The critical soil moisture content, θ_c , defines the point at which the crop's transpiration rate begins to rapidly decline with decreasing soil moisture. Maximum allowable depletion, MAD , is defined as the ratio of RAW to AW and can be estimated for various crops from the literature (Table 5.4). Management parameters MAD , fc , and pwp are difficult to precisely determine for a given crop system and so conservative values must be used to avoid crop stress.

Table 5.4 Irrigation management parameters for various crops

Crop	D_{rz}		MAD	
	James ¹	SCS ²	James	SCS
Spring grain	90 cm	120 cm	0.65	0.50
Winter grain	90	120	0.65	0.50
Sugar beets	105		0.65	
Beans, dry	90	90	0.50	0.50
Corn, sweet	120	90	0.65	0.40
Corn, field	120	120	0.65	0.50
Onions	60	30	0.50	0.35
Potatoes	60	90	0.30	0.35
Alfalfa	180		0.65	

¹ James, 1988.

² Soil Conservation Service Engineering Handbook, 1984.

Under a water budget irrigation scheduling regime, daily evapotranspiration losses (ET) are measured or estimated. This ET loss is subtracted from readily available water until *RAW* is fully depleted at which point irrigation is required. The soil-water budget method was used in this research to determine irrigation water requirements, Z_{req} , for each irrigation.

The available water capacity (*AWC*) is the depth of water held by a unit depth of soil. The total depth of available water (*AW*) may be determined by multiplying the available water capacity, *AWC*, by the effective root zone depth, D_{rz} . Some regional soil properties may be found in Table 5.5 which lists the

most common soil series and respective available water capacities found in northeast Malheur County (USDA SCS, 1984).

Table 5.5 Soil series and available water capacities (AWC)

Soil series	Range (cm cm ⁻¹)	% of survey area*
Ahtanum silt loam	0.10 - 0.21	0.4
Feltham loamy fine sand	0.05 - 0.09	0.8
Garbutt silt loam	0.18 - 0.20	2.5
38 to 62 inches	0.11 - 0.13	
Greenleaf silt loam	0.17 - 0.21	3.0
Kimberly fine sandy loam	0.11 - 0.17	1.3
Nyssa silt loam	0.17 - 0.21	12.9
Owyhee silt loam	0.19 - 0.21	9.0
28 to 60 inches	0.14 - 0.18	
Powder silt loam	0.18 - 0.25	6.6
Quincy loamy fine sand	0.06 - 0.09	0.6
Sagehill fine sandy loam	0.20 - 0.23	0.9
Truesdale fine sandy loam	0.09 - 0.15	0.5
Turbyfill fine sandy loam	0.12 - 0.14	3.9
Virtue silt loam	0.19 - 0.21	7.7

*Figures for soil series of slope 0 to 5 percent.

Source: USDA SCS/OSU Experiment Station, Northeast Malheur County Soil Survey, 1983.

5.10 Irrigation efficiency and distribution uniformity

Irrigation *application efficiency* (AE) is defined as the ratio of the volume of water beneficially used, V_{bu} , to the total water applied (ASCE, 1978). Equation 32 yields *application efficiency* as a percentage.

$$AE = \frac{V_{bu}}{V_{applied}} 100 \quad (32)$$

The leaching fraction may be included in the volume of water which is beneficially used and therefore becomes part of the *application efficiency* equation. *Irrigation efficiency*, defined as the ratio of the volume of water stored in the root zone to the volume of water applied is equal to AE when the leaching fraction is zero and when conveyance losses are negligible.

Distribution uniformity (DU) is the average low-quarter depth of infiltration, Z_{lq} , divided by the field averaged depth of water infiltrated, defined as Z_{avg} (ASCE, 1978).

$$DU = \frac{Z_{lq}}{Z_{avg}} 100 \quad (33)$$

Another important term is *irrigation adequacy* (A) or percentage of field adequately irrigated. This is especially important to furrow irrigation systems due to the differences in intake opportunity time between the top and bottom of the field. Irrigation adequacy is calculated by dividing the area of the field which is fully irrigated (minimum depth of Z_{req}) by the total irrigated area.

5.11 Model calibration

The objective of model calibration is to ultimately be able to accurately predict the distribution of infiltrated water along the furrow. The work in this thesis presents two modes of operation for the SRFR model. First, “average” or representative parameters for intake, roughness and furrow cross-sections are presented for use with SRFR in Sections 6.1, 6.2, and 6.3. These parameters are meant to be general guidelines for the evaluation of irrigations given “average” field conditions. Secondly, procedures are outlined in this section for calibrating the SRFR model for a particular irrigation event, so that various irrigation strategies may be evaluated for these specific conditions. The representative values for intake, roughness and furrow cross-section (from Sections 6.1-6.3) may be used to begin the calibration process.

Ideally, model calibration would be achieved by matching simulation infiltrated profiles to that observed in the field. Smerdon et al. (1988) cites the difficulties in accurately measuring the subsurface distribution of water because of the large number of observations required. The nonuniformity of initial conditions, intake and possible interference from adjacent irrigated furrows makes this a difficult task.

An alternative method of model calibration consists of: (1) fitting simulation advance data to observed advance data; and (2) matching inflow and outflow volumes (a mass balance).

For calibration of a kinematic wave model, equation 34 was used by Izadi

et al. (1991). No absolute criteria were established except that the sum of residuals squared value (*SRES*) was minimized by varying the intake coefficients.

$$SRES = \sum |T_s(x_i) - T_m(x_i)| \quad (34)$$

Variable *SRES* is the sum of the absolute values of the residuals, x_i is advance distance to node *I*, $T_s(x_i)$ is simulated time of advance to distance x_i , and $T_m(x_i)$ is the observed time of advance to distance x_i . Due to the variability of field conditions, values of *SRES* increase with greater advance times. Because of this, the *SRES* value must be normalized so that the "goodness of fit" for each irrigation simulation is comparable. It is proposed here that a modified measure of fit be used,

$$NSRES = \frac{SRES}{t_i} \frac{1}{n} \quad (35)$$

where *NSRES* is the normalized sum of residuals, t_i is the field observed time of completion of advance, and n is the number of observations from an irrigation event. The criterion used to determine a good fit to field advance data is the arbitrarily chosen *NSRES* value of 0.04 or less. Based on experience, this value roughly represents the balance between a time consuming search for a near-perfect least squares fit and the swifter yet subjective method of graphical comparisons. Though advance curves are typically non-linear, no weighting factors or transformations were used for different stages of advance. This is

because of the ultimate desire to accurately predict intake opportunity times near the tail end of the field.

To complete the calibration, simulation volumes of furrow runoff, V_{pred} , are closely matched to field observed runoff volumes, V_{obs} . The second criterion used to calibrate the SRFR model, the normalized difference in predicted and observed runoff, V^* , should not exceed an arbitrarily chosen 10 percent.

$$V^* = \frac{V_{pred} - V_{obs}}{Q_o t_{ro}} \quad (36)$$

The maximum error in the average depth of infiltration, ϵ_{DI} , is then equal to

$$\epsilon_{DI} = \frac{0.10 V_T}{LW} \quad (37)$$

where L is furrow length, W is irrigated furrow spacing and V_T is total inflow volume and is equal to $Q_o t_{ro}$ where t_{ro} is the elapsed time at which the runoff volume is measured and the inflow shut off. This criterion works well for assuring an accurate relative distribution between runoff and infiltration. The actual runoff hydrograph may, nevertheless, differ some from that observed in the field. Blair and Smerdon (1988) used the normalized difference in predicted and observed runoff (equation 36) as a criterion for testing several solutions to the Lewis and Milne surface irrigation volume balance equation. Using field data from published experiments, they found normalized differences to average 2.8 to 6.7 percent. No maximum difference criteria were established.

The computer model, SRFR, is not currently suited for multiple iterative

runs to optimize the infiltration and roughness parameters for a given data set. This is mainly due to the lengthy execution time for a single simulation. Because of the absence of a means for an iterative solution, the calibration procedure proposed is partly subjective. This procedure is always to be used in conjunction with field measurements from a specific irrigation event. The SRFR calibration procedure is summarized below:

1. Determine field slope(s) and furrow cross-sectional geometries from field measurements.
2. Determine if the field needs to be segmented for the simulation based on breaks in slope and abrupt changes in physical conditions.
3. Calculate mean inflow rate, Q_o .
4. Estimate Manning roughness, n , from research data or field experience.
5. Estimate intake coefficient, b , from furrow flow data, if available, or from Table 6.1.
6. Estimate intake coefficients k , a and c based on tractor traffic from Table 6.1. Divide intake coefficients k , b , a and c from equation 3 by an estimate of the mean wetted perimeter, P , to obtain SRFR intake coefficients.

$$Z_n = \left(\frac{k}{P}\right)\tau^a + \left(\frac{b}{P}\right)\tau + \left(\frac{c}{P}\right) \quad (38)$$

7. Run SFR simulation.
8. Record simulation advance times for each station, $T_m(x_i)$.
9. Calculate normalized sum of residuals squared, $NSRES$.
Determine if $NSRES < 0.04$.
10. Record runoff volume and normalized difference between predicted and measured, V . Is the normalized difference less than 10 percent?
11. If the fit is not satisfactory, revise estimates of k , a and c . A slight modification of b may be required also. Go to step 7.

6. RESULTS

6.1 Furrow intake observations

Measured intake curves are presented in terms of cumulative volume of water infiltrated per unit length of furrow (L^3L^{-1}). Long term or "basic" furrow intake rates are in terms of volume infiltrated per unit length of furrow per unit time ($L^3L^{-1}T^{-1}$).

6.1.1 Average intake curves

Generalized cumulative intake curves were derived for non-wheel and wheel traffic compacted furrows from inflow-outflow data (Figure 6.1). Data obtained from recirculating infiltrometer tests were not used because of the relatively short duration of these tests (8 hours or less) compared to 24 hours for most irrigation events. Data from four farm sites were used to derive the representative non-wheel traffic intake curve. These locations are the Barlow farm (winter wheat field), Bel-Air Farms and Fields B3 and B7 at the OSU Malheur Experiment Station. The total number of non-wheel traffic curves used are four (one from each of the sites). To develop the representative intake curve for wheel traffic compacted furrows, intake data from the same four sites were used. The total number of wheel traffic curves are four.

The Extended Kostiakov equation (equation 3) was chosen to model the

generalized cumulative intake curves because of the wide range of intake curve shapes and its compatibility with SRFR. To fit the data, an optimizer function within the spreadsheet program was used to minimize the sum of residuals squared between 0 and 25 hours intake opportunity time. For non-wheel traffic furrows, long term rates (approximated by the b term of equation 3) were constrained to no less than $3.0 \text{ l m}^{-1}\text{h}^{-1}$. Similarly, for wheel traffic compacted furrows, rates were constrained to values of no less than $1.0 \text{ l m}^{-1}\text{h}^{-1}$.

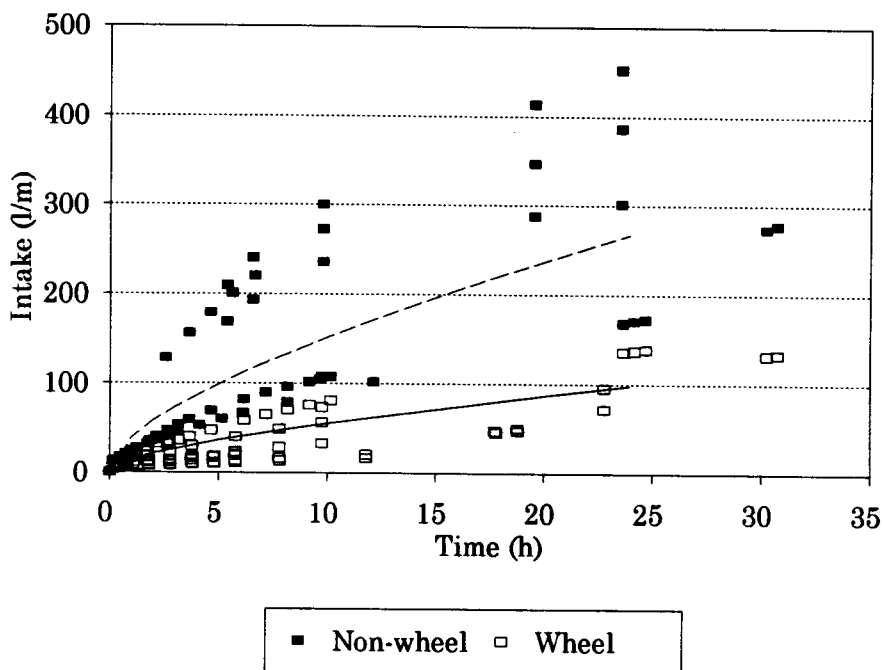


Figure 6.1 Representative cumulative intake curves for bare non-wheel and wheel traffic furrows derived from inflow-outflow data. Data points from each intake test are also presented. These data are from the Barlow farm, Bel-Air Farms, and Fields B3 and B7 at the OSU Malheur Experiment Station.

Table 6.1 Average intake coefficients to $Z=kt^a+bt+c$

Furrow type	k $l\ m^{-1}\ h^{-a}$	a	b $l\ m^{-1}\ h^{-1}$	err* %
Non-wheel	36.	0.50	3.9	45.
Wheel	13.	0.48	1.7	44.

*Average absolute error.
Intake parameter c is assumed to = 0.

The generalized intake curves in Figure 6.1 show that approximately $150\ l\ m^{-1}$ were infiltrated after 10 hours intake opportunity time for the non-wheel traffic furrow. In contrast, approximately $50\ l\ m^{-1}$ were infiltrated after 10 hours opportunity time for the average wheel traffic furrow. Furthermore, the figure shows that furrow intake data varies for both non-wheel or wheel traffic compacted furrows. This is also reflected by the average absolute error, shown in Table 6.1, for each generalized intake curve. The average absolute error, in percent, is defined as follows:

$$err = avg\left[\frac{abs(predicted - measured)}{measured}\right]100 \quad (39)$$

An average absolute error of 45% was calculated for non-wheel traffic furrows and 44% for wheel traffic compacted furrows.

The average intake coefficients to the Extended-Kostiakov equation for non-wheel and wheel traffic compacted furrows are given in Table 6.1. These are the recommended intake curves to be used with the SRF model. It is

recognized that these intake curves are only general guidelines based on a limited number of observations and that these curves represent “average” conditions. Prior to being used with SRF, recall that the intake coefficients must first be converted to depth units ($L T^{-1}$) by dividing them by an estimate of the mean wetted perimeter, P (Section 5.11, equation 38).

Initial soil moisture, soil texture, previous number of irrigations and such variables as field slope and inflow rate are all physical factors that partly determine furrow intake rate (Section 4.1). This research solely presents findings based on the presence (or not) of wheel traffic compaction. This appears to be the single most important factor. Unfortunately, sufficient data were not available to further categorize intake curves based on the aforementioned factors. Of practical importance though, there are some limitations which restrict the researcher’s ability to successfully categorize empirical furrow intake curves based on the above variables. These being the limited precision of field scale data, the extensive inter-relationships which exist between physical parameters and lastly, variability which cannot be explained.

6.1.2 Long term intake rates

Long term intake rates from several farm sites are shown versus wetted perimeter for wheel traffic and non-wheel traffic furrows (Figure 6.2). Measured wetted perimeters range from 8 cm for steeply sloped bare furrows to

over 30 cm for straw mulched furrows. Long term intake rates ranged from 0.50 to over 10 l m⁻¹ h⁻¹ (0.0054 to 0.11 ft³ft⁻¹h⁻¹). To test for a correlation, a straight-line relationship was fit to both wheel and non-wheel traffic data sets and the resulting coefficient of determination values (r^2) were 0.26 and 0.48 respectively. Though a correlation cannot be dismissed, these data show no well-defined relationship for either non-wheel traffic or wheel traffic compacted furrows. Presumably, infiltration becomes increasingly one-dimensional as lateral water movement decreases late in the irrigation. Increases in long term furrow intake rate with wetted perimeter would therefore be relatively small though wetted perimeter may have a more important effect on intake early in the irrigation.

Table 6.2 Mean intake values and standard deviations

Furrow type	No. obs.	Mean l m ⁻¹ h ⁻¹	Std. dev. l m ⁻¹ h ⁻¹
Non-wheel	24	5.6	2.3
Wheel	27	3.0	1.3
Non-wheel straw	3	7.2	2.9
Wheel straw	8	2.8	1.1

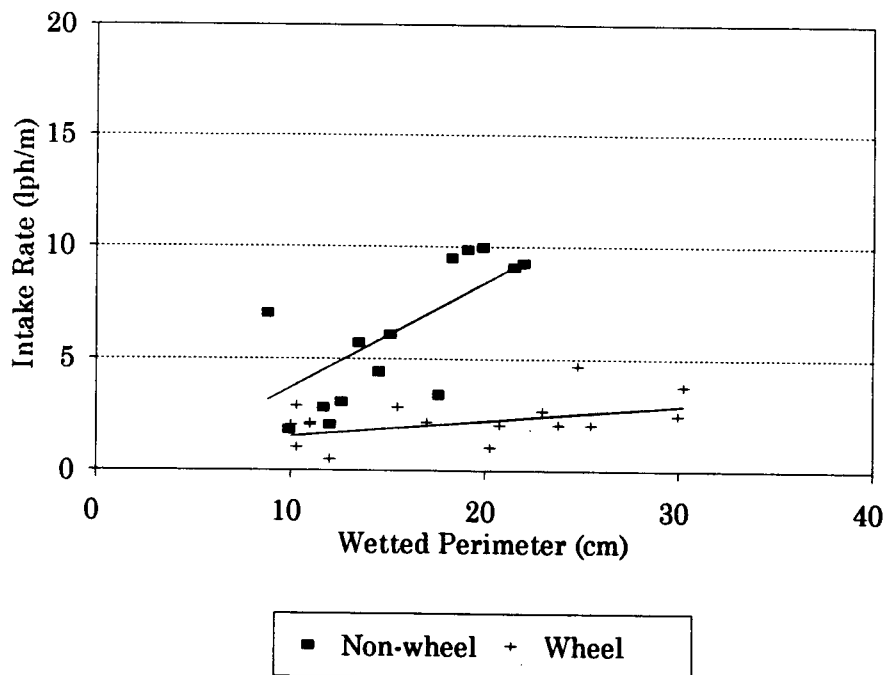


Figure 6.2 Long term intake rates for non-wheel and wheel traffic compacted furrows versus stream wetted perimeter. These data are from several farm sites throughout northeast Malheur County including the OSU Malheur Experiment Station.

There were 24 independent observations of long term intake rate in non-wheel traffic furrows, 27 observations in wheel traffic furrows, 3 in non-wheel strawed furrows and 8 in wheel traffic strawed furrows. The averages and standard deviations are presented in Table 6.2. Mean intake values of non-strawed non-wheel traffic furrows were approximately 87 percent greater than for wheel traffic rows. The mean intake values for bare furrows were statistically tested using the Student's *t* distribution. The *t* statistic was calculated to be 4.95, resulting in a greater than 99% confidence level that the

mean values are statistically different.

The significance of this discussion with regards to SRFR is two-fold. First, the long term intake rate, roughly represented by coefficient b of the Extended-Kostiakov equation, greatly determines the performance of an irrigation. More specifically, it has important bearing on the ultimate distribution of water down the furrow and likewise, the runoff hydrograph. Secondly, because long term intake rates do not increase greatly with stream wetted perimeter, the importance of modeling infiltration as a function of wetted perimeter decreases as steady conditions are achieved during the irrigation.

6.2 Manning's roughness and channel section factor

Manning's roughness was calculated from direct measurements of flow rate, flow depth, slope, and furrow shape. Calculated values of Manning's roughness varied from a low of 0.03 to a high of 0.14 for non-strawed furrows and up to 0.36 for straw mulched furrows. Table 6.3 presents the results from each irrigation event. These results are summarized in Table 6.4 which gives recommendations based upon furrow condition at the time of irrigation.

Table 6.3 Manning's roughness for each irrigation event

Field	Date	Crop	Irrig. No.	Manning's n
MES B7*	4/05/94	w. wheat	1	0.08
MES B7*	4/26/94	w. wheat	2	0.09
Bel-Air Farms	4/12/94	w. wheat	1	0.03
Barlow farm	5/10/94	w. wheat	2	0.04
Duyn farm	9/03/93	sugar beets	>5	0.12†
Barlow farm	4/11/94	sugar beets	1	0.04
MES B3*	6/01/94	potatoes	1	0.10 0.36**
MES B3*	6/09/94	potatoes	2	0.06 0.18**
MES B3*	6/15/94	potatoes	3	0.045 0.30**
MES B3*	6/22/94	potatoes	4	0.06 0.15**

* O.S.U. Malheur Experiment Station.

**Straw mulched furrows.

† Vegetative interference.

Table 6.4 Recommended Manning's n values

Furrow condition	Range	Mean	No. obs.
Bare soil	0.03 to 0.12	0.06	21
Vegetative interference	0.09 to 0.14	0.12	2
Straw mulched	0.18 to 0.36	0.27	6

The calculation of Manning's roughness coefficient, n , shows some sensitivity to errors in flow depth measurement. This sensitivity was studied using data from Fields B3 and B7 at the Malheur Experiment Station. Based on the furrow geometry and slope of Field B3 (assumed channel side-slope $z = 2.00$, bed-width $b = 14.5$ cm and field slope = 0.030), Manning's n values were calculated for several flow depths and inflow rates. It can be seen in Figure 6.3 that for a given flow rate, a large range of Manning's n values may be calculated from small errors in stream depth measurement. For Field B7 (assumed channel side-slope $z = 1.50$, bed-width $b = 6.1$ cm and field slope = 0.0055), calculations of Manning's n from stream depth measurement were found to be less sensitive to error, as seen in Figure 6.4. This difference in sensitivity is largely due to field slope. As field slope increases, the normal depth, y_n , decreases, and the influence of flow variables on flow depth decreases.

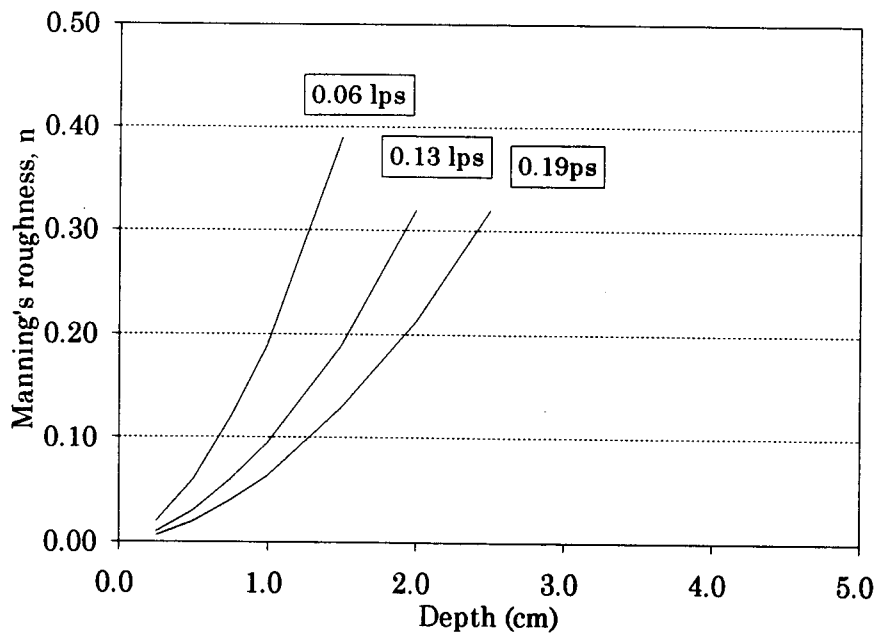


Figure 6.3 Normal depth as a function of Manning's roughness for several inflow rates given the field slope and furrow shape of Field B3 potatoes. Field slope is 0.030, side-slope $z = 2.00$ and channel bed-width $b = 14.5$ cm. O.S.U. Malheur Experiment Station, Ontario, Oregon, 1994.

Stream wetted perimeter, P , may be predicted from channel section factor estimates. Figure 6.5 shows wetted perimeter as a function of section factor, F , for several fields, assuming uniform flow conditions. The section factor was calculated using equation 12 (same as equation 40) from estimates of Manning's n , slope, S_o , and inflow rate, Q_o . These results show a similar relationship to data presented by Trout (1991). Trout presents wetted perimeter versus section factor data from field observations in Idaho and Colorado. He found that the relationship follows a power curve with a rapidly decreasing slope as section

factor increases. The coefficients to the power function, $P = cF^e$, are given in Table 6.5 for Idaho and Colorado and from northeast Malheur County data. The fitted power curve relationship may be used to estimate wetted perimeter for a given section factor.

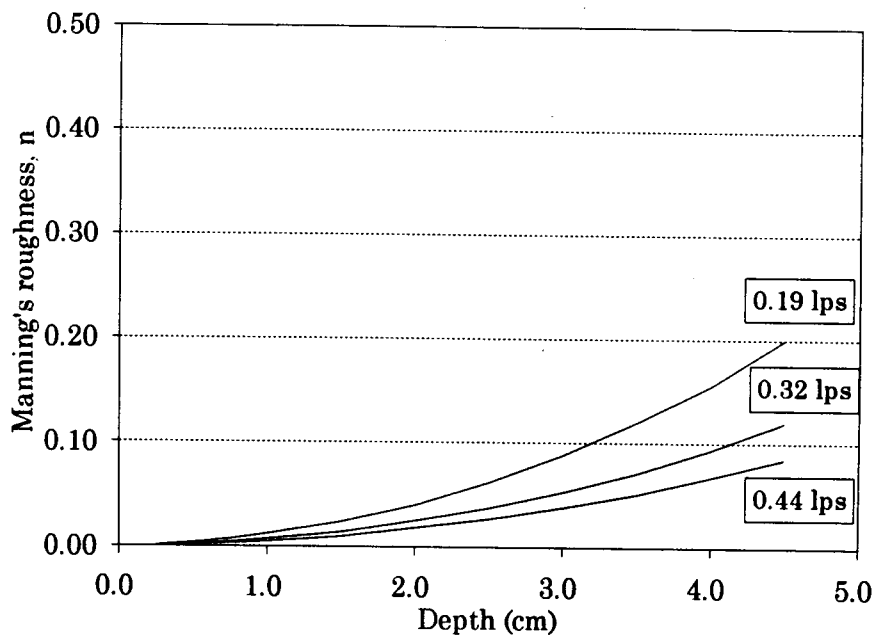


Figure 6.4 Normal depth as a function of Manning's roughness for several inflow rates given the field slope and furrow shape of Field B7 spring wheat. Field slope is 0.0055, side-slope $z = 1.5$ and channel bed-width $b = 6.1$ cm. O.S.U. Malheur Experiment Station, Ontario, Oregon, 1994.

Data from straw mulched furrows appears to deviate from the data for bare soil conditions. Figure 6.5 shows that given a particular section factor value, greater wetted perimeters are observed for the straw mulched potato furrows. Solving the Manning equation in terms of section factor,

$$F = \left(\frac{A^{5/3}}{P^{2/3}} \right) = \left(\frac{Qn}{\sqrt{S_o}} \right) \quad (40)$$

it can be seen that F is fixed for a given flow rate, field slope and hydraulic roughness and likewise for a given flow depth. Consequently, the relationship between flow depth and wetted perimeter determines the section factor curve. Though straw mulching increases Manning's roughness, more importantly, straw mulching preserves the original furrow shape, and therefore the relationship between flow depth and wetted perimeter.

Table 6.5 Wetted perimeter vs. section factor regression coefficients to $P=cF^e$ (units in cm)

Location	c	e	err**
Colorado*	8.37	0.23	10%
Idaho*	6.30	0.24	10
Malheur Co. 1993-94	4.92	0.34	15

* Trout, 1991.

**Average absolute error.

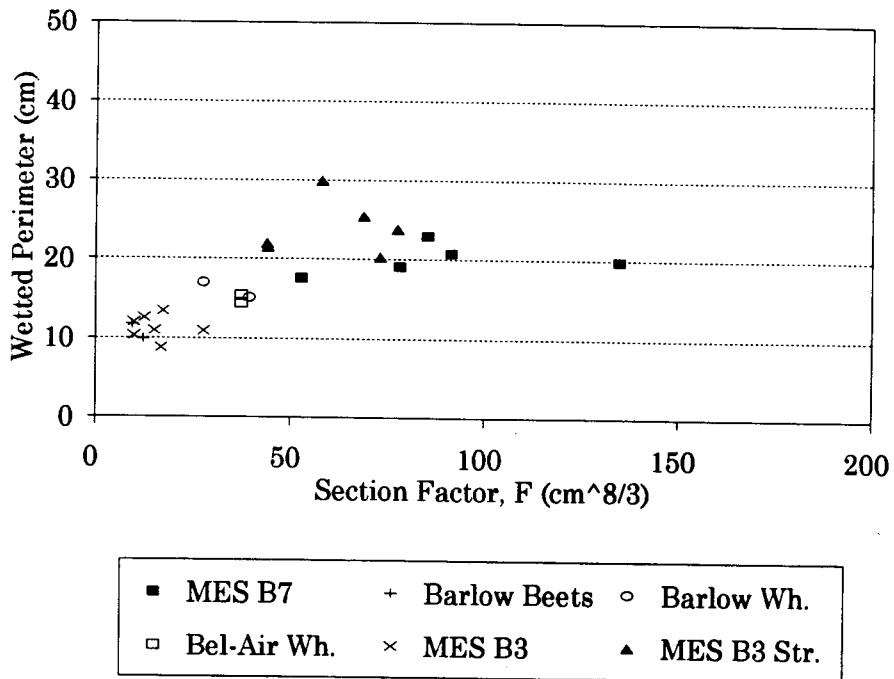


Figure 6.5 Wetted perimeter, P , versus furrow section factor, F , from several irrigations events during 1993 and 1994. Parameter F was calculated from the Manning equation using estimates of Manning's n , inflow rate, Q_o and field slope, S_o .

6.3 Furrow channel geometry

This section presents results from channel profile measurements using the profilometer. A summary is given of recommended furrow bed-widths and side-slopes for various crops and conditions for use within the SRFR model. Following this, several graphs are presented of selected furrow channel shapes from different crop systems and field configurations.

6.3.1 Furrow geometry summary

Furrow shape early in the season is typically determined by the size of the shovel (fastened to the drawbar) used to create the furrow. Typical furrow spacings are 51, 56, 76 and 91 centimeters (20, 22, 30 and 36 inches) and are usually chosen for a particular crop. Depending on tractor and implement configuration, and the amount of overlap, wheel traffic compacted furrows commonly are every other, every third, or every fourth furrow.

Changes in furrow shape throughout the irrigation season are difficult to quantify due to the many measurements required and number of parameters involved. For this reason, graphical representations of selected furrow shape measurements are presented and discussed qualitatively in Section 6.3.2. The approximation of furrow shape by a trapezoid, according to profilometer measurements, provides a crude yet practical method by which flow-depth relationships can be established. Moreover, the trapezoid model can encompass a wide range of furrow sizes and shapes.

A breakdown is given in Table 6.6 of profilometer results from each irrigation event. The channel bottom width, b , is given along with the channel side-slope, z . From these data, recommendations for furrow shape parameters were calculated by averaging the results (Table 6.7) according to the size of the furrow. Furrows are arbitrarily classed as small, medium and large. The size of the furrow is largely determined by the crop planted because of differences in

cultural practices. These recommended values are for use with the SRFR model. It should be recognized that for extreme cases, such as severe erosion of the furrow channel, these recommendations are not valid.

Table 6.6 Furrow channel dimensions from profilometer results

Farm	Crop	Date	Channel bottom width <i>b</i> cm	Side-slope <i>z</i> cm cm ⁻¹
MES B7	grain	5/11/93 NW	6.0	1.40
		5/11/93 W	6.2	1.53
		6/30/93 NW	7.0	1.52
		6/30/93 W	13.0	1.44
		8/27/93 NW	6.3	1.43
		8/27/93 W	11.9	1.60
Cruick.	corn	7/30/93 NW	8.5	1.67
		7/30/93 NW	13.0	1.50
Duyne	beets	9/03/93 NW	12.0	1.54
		9/03/93 W	14.5	1.00
Bel-Air	grain	4/12/94 NW	4.7	1.47
		4/12/94 W	3.0	2.00
		4/21/94 W	5.1	1.55
Barlow	beets	5/11/94 W	3.9	2.03
Barlow	grain	6/03/94 NW&W	6.8	1.24
MES B3	potatoes	5/31/94 W	4.0	2.62
		5/31/94 W ST	6.3	2.33
		6/14/94 W	4.8	0.98
		6/14/94 W ST	14.5	2.00
		6/14/94 NW	4.7	1.74
		6/14/94 NW ST	7.0	2.75
W	wheel traffic.			
NW	non-wheel traffic.			
ST	strawed.			
NST	non-strawed.			

Table 6.7 Recommended furrow geometries

Furrow size	Channel bottom width <i>b</i> cm	Side-slope <i>z</i> cm cm ⁻¹
Small furrows: beans, onions	4.0 cm	2.0
Medium sized furrows: grain, beans, onions, beets, corn	6.5	1.5
Large furrows: potatoes, corn	9.5	1.8

Furrow shape and size can vary significantly from field to field and from irrigation to irrigation as can be seen in Table 6.6. Even so, it was found that a strong linear relationship exists between wetted perimeter, P , and flow top width, T (Figure 6.6). A first order equation fit to the data yields the following relationship with a coefficient of determination (r^2) of 0.98.

$$P=1.67+1.067T \quad (41)$$

For each furrow, the wetted perimeter and top width data are the average of several measurements made along a section of furrow late in the irrigation. Assuming that a trapezoid adequately represents furrow shape, it can likewise

be shown in the following equation, that a linear relationship exists between wetted perimeter and flow top width, T , when b and z are constant for a given furrow.

$$P = b + \left(\frac{T-b}{z}\right)\sqrt{1+z^2} \quad (42)$$

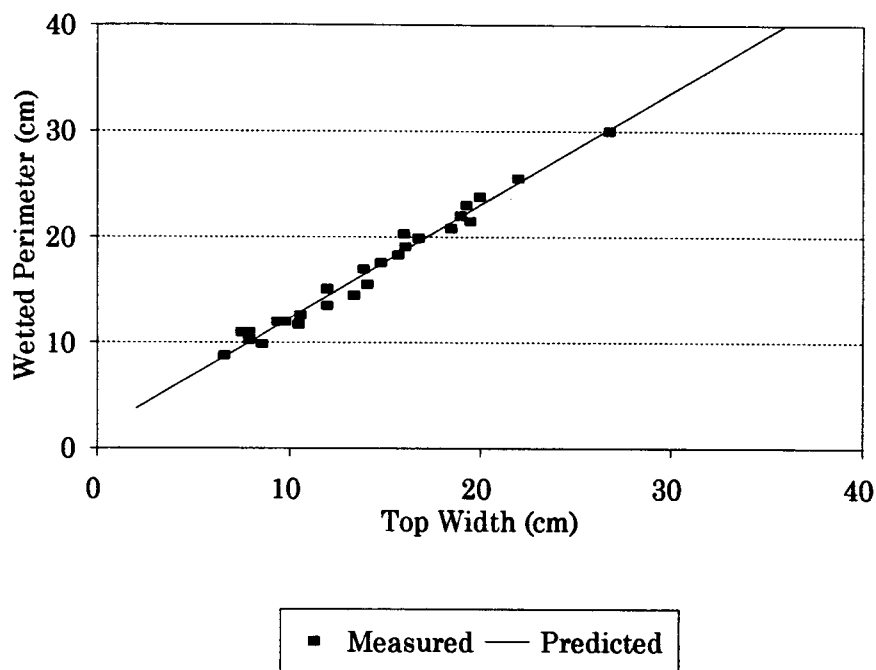


Figure 6.6 Stream wetted perimeter, P , versus top width, T . Data are from several irrigation events observed during 1994 at the OSU Malheur Experiment Station and at several off-station sites.

6.3.2 Selected furrow cross-sections

This section gives a qualitative discussion of furrow cross-sectional shape and presents several examples from the many profilometer measurements. It is important for the researcher to have a practical understanding of how furrow channels may evolve during the course of the growing season. When fitting the SRFR model to data from an irrigation event, the shape of the channel at the time of irrigation must be considered. These few examples provide the means for a discussion of furrow cross-sections for different crop systems and field conditions.

Two potato furrows from Field B3 at the Malheur Experiment Station are shown in Figure 6.7. One furrow was treated with straw mulch (940 lb ac^{-1} or 1050 kg ha^{-1}) and the other was not treated. The slope on this field was near 3.0 percent and the furrow inflow rate was relatively low at 0.19 l s^{-1} (3 gpm). The untreated furrow had a deeply eroded channel while the straw mulched furrow remained broad and shallow. This erosion of the furrow channel decreases the wetted perimeter of the stream and therefore intake area. Conversely, the straw-mulch treatment preserves furrow shape throughout the irrigation season maintaining a wide and shallow channel.

Observable changes in furrow cross-section may also occur on shallower sloped fields. Figure 6.8 shows a non-wheel traffic furrow cross-section from Field B7 at the Malheur Experiment Station prior to the first irrigation (May 11, 1993) and then prior to harvest (August 27). These cross-sections were

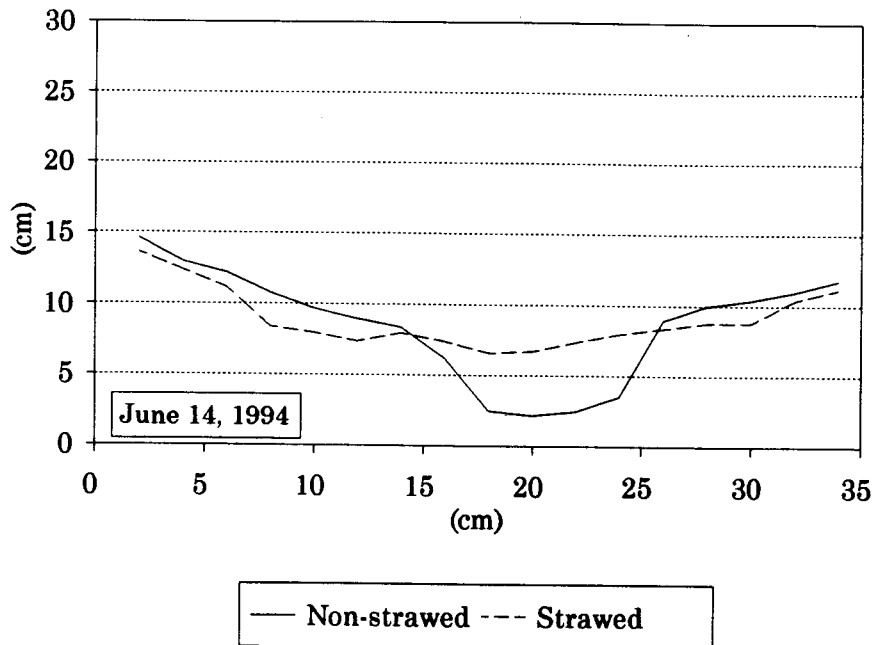


Figure 6.7 Furrow cross-sections from MES Field B3 for a non-straw and straw mulched furrow after one irrigation. Field slope is approximately 3 percent and the soil is a Nyssa silt loam. OSU Malheur Experiment Station, Ontario, Oregon, 1994.

measured at 20 m (60 ft) from the top of the field. Furrows in shallow sloping fields (in general, field slopes of less than 0.50%) tend to become increasingly wider with each irrigation as sediments settle out and as the stream cuts into the furrow bank. This field was planted to spring wheat where the density of the crop stand helped to stabilize furrow shape. Nevertheless, some broadening of the furrow channel can be observed.

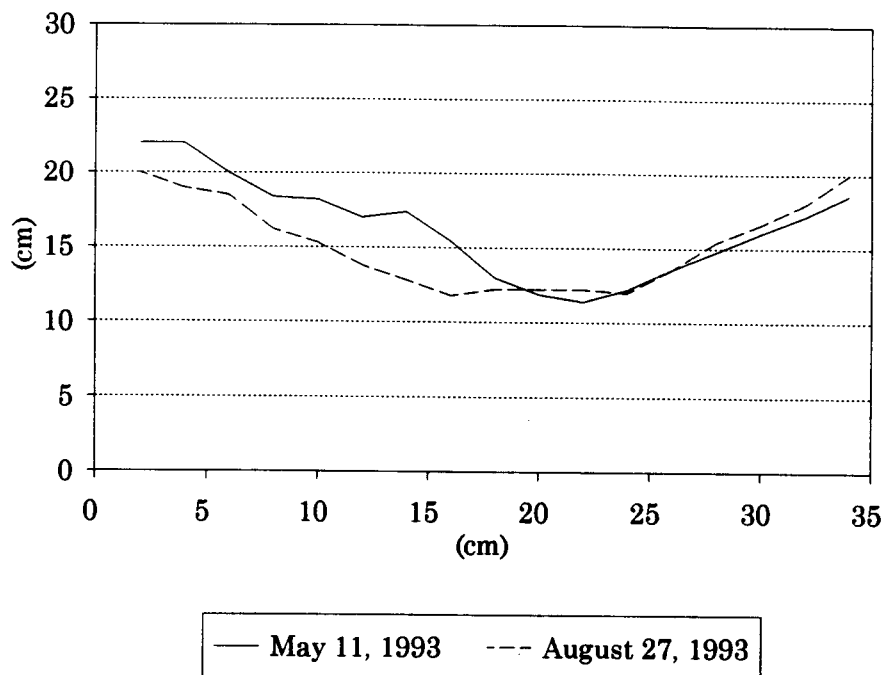


Figure 6.8 Furrow cross-sections from MES field B7 for a non-wheel traffic furrow prior to the first irrigation (May 11, 1993) and prior to harvest (August 27, 1993). Field slope is approximately 0.5% and the soil is a Greenleaf silt loam. OSU Malheur Experiment Station, Ontario, Oregon, 1994.

Furrow spacings are often standard for a given crop though shovel size and shape used to cultivate may vary. Figure 6.9 shows furrow cross-sections from the Cruickshank corn field before and after the July 22, 1993 irrigation. The Cruickshank field had a 0.60 percent slope and was planted to corn on 30 inch (0.76 m) centers. These furrows were created with a larger shovel size than those used to cultivate MES Field B7 (Figure 6.7).

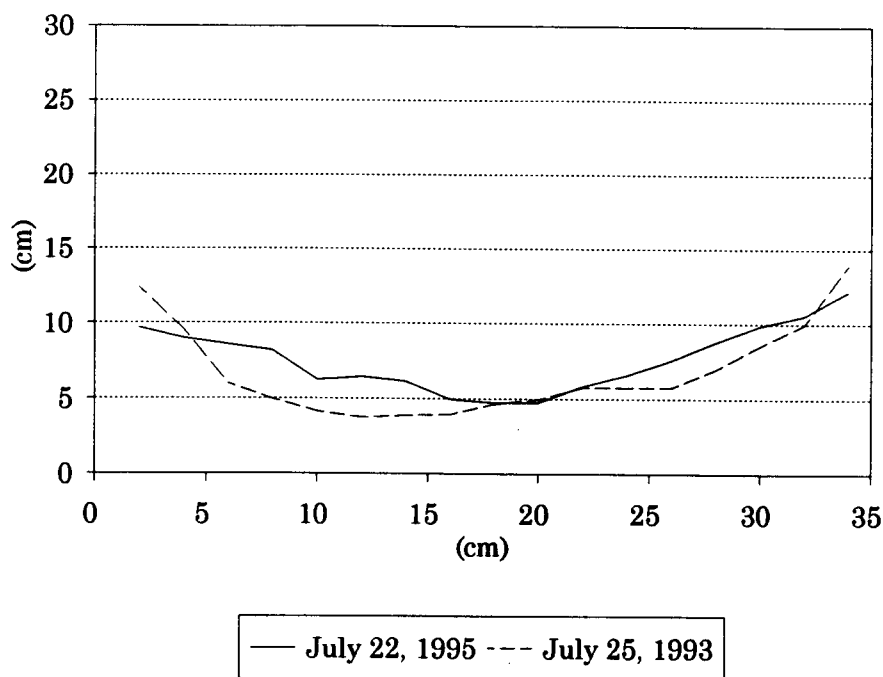


Figure 6.9 Furrow cross-sections from the Cruickshank farm planted to corn. Cross-sections are from July 22 and July 25, 1993 prior to and after an irrigation following cultivation. The field slope is near 0.6% and the soil is an Owyhee silt loam.

The cross-sectional shape of wheel traffic compacted furrows on moderate to steeply sloped fields may evolve more rapidly than non-wheel furrows. The low intake of wheel traffic furrows results in greater stream velocities and higher erosion rates. Figure 6.10 shows two furrow cross-sections from a sugar beet field in early September. Irrigated furrow spacing for this field was 44 inches (1.12 m) on-center and the field slope averaged 0.9 percent but varied down the length of the furrow. The furrow cross-sections pictured were measured near the tail of the field where the slope was near 1.2 percent. The

non-wheel traffic furrow cross-sections for both the top and bottom of the field were similar, showing a wide, shallow channel. In comparison, the wheel traffic furrow cross-section shows a much narrower channel due to the high velocity and erosivity of the runoff water. The opportunity time for erosion is greater in wheel traffic furrows due to the lower permeability and rapid advance.

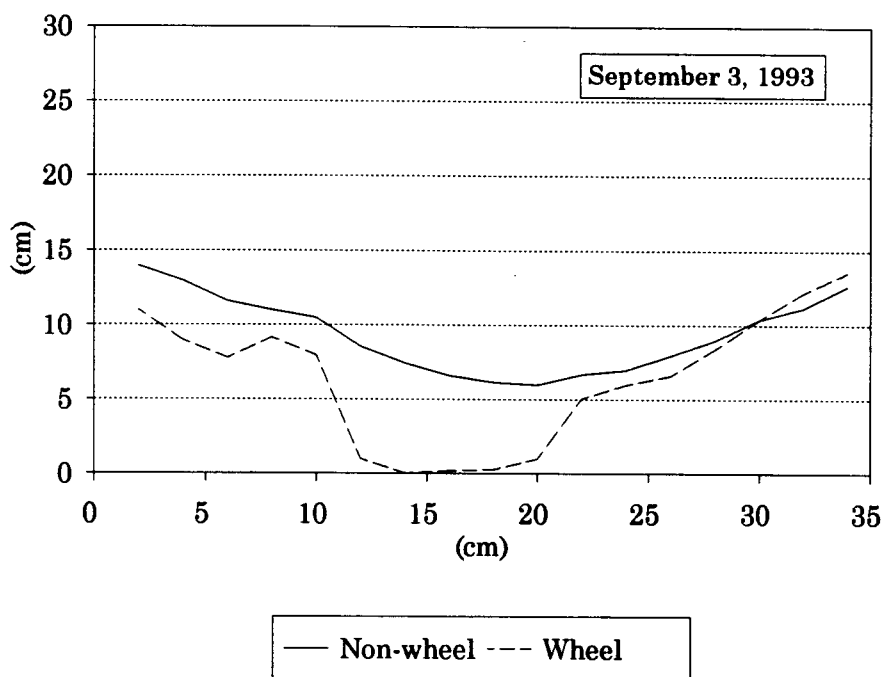


Figure 6.10 Wheel and non-wheel traffic furrow cross-sections from the Duyn sugar beet field, September 3, 1993. Cross-sections are from the tail of the field, at 274 m. Field slope averaged 0.9% and the soils is a Feltham loamy fine sand.

6.4 Calibration of the SRF model with field data

This section presents SRF simulations of several irrigation events in northeast Malheur County during 1993 and 1994. SRF was calibrated

specifically for each irrigation event using field data from that event. The result is a set of several different calibrated versions of the model, each of which is regarded as valid only for that specific event. The purpose of this exercise was to evaluate, qualitatively, how well SRFR is able to approximate actual irrigation events and to illustrate the performance of furrow irrigation systems in northeast Malheur County. Ultimately, these several calibrated versions may be used to estimate how changes in irrigation practices would have effected water distribution for these specific events.

The procedure used to calibrate the SRFR model is outlined in Section 5.11. Simulation results include stream advance times and infiltrated water distribution along the furrow. Graphical comparisons of SRFR simulation results with field observations are presented for four irrigation events. These figures show advance times and the infiltrated water profile along the furrow as determined by flow measurements and neutron probe soil moisture data.

Estimates of furrow geometry, field slope, intake characteristics and hydraulic roughness are required inputs for each simulation in addition to irrigation set time, inflow rate(s) and required irrigation depth. SRFR requires furrow intake coefficients to be in terms of volume per unit area of wetted perimeter per unit time ($L \cdot T^{-1}$). With regard to the intake coefficients, it is recommended by this researcher that the exponential α term of the Extended Kostiakov intake equation be no less than 0.40 due to computational difficulties. Values of α from previous research range from 0.0 to 0.80 (Elliott et al., 1983b;

Walker and Humpherys, 1983; Blair and Smerdon, 1988). Output from SRFR include irrigation advance times, the outflow hydrograph, distribution of infiltrated water, various field averaged performance values and calculations of irrigation efficiency, uniformity and irrigation adequacy.

Irrigations are identified by farm site, date of irrigation and furrow type (wheel traffic or non-wheel traffic, strawed or non-strawed). SRFR irrigation simulations are identified in Table 6.9 along with the calibration parameters: normalized sum of residuals squared, *NSRES*, and normalized runoff volume error, V^* , which are from equations 44 and 45 respectively:

$$SRES = \sum |T_s(x_i) - T_m(x_i)| \quad (43)$$

$$NSRES = \frac{SRES}{t_l} \frac{1}{n} \quad (44)$$

$$V^* = \frac{V_{pred} - V_{obs}}{Q_o t_{ro}} \quad (45)$$

Table 6.8 SRFR simulations and calibration fitting parameters

Farm ID	Date	<i>NSRES</i> ¹	<i>V</i> ²	Model
MES B7 W	5/11/93	0.014	0.019	ZI
MES B7 NW	5/11/93	0.011	0.000	ZI
MES B7 W	6/14/93	0.021	0.050	ZI
MES B7 NW	6/14/93	0.035	0.060	ZI
Bel-Air W	4/12/94	0.033	0.011	ZI
Bel-Air NW	4/12/94	0.035	0.000	ZI
Duyn W	9/03/93	0.025	0.002	ZI
Duyn NW	9/03/93	0.020	0.007	ZI
Cruickshank NW	7/22/93	0.019	0.002	ZI
MES B3 W ST	6/01/94	0.040	0.021	KW
MES B3 W NST	6/01/94	0.026	0.007	KW
MES B3 NW ST	6/09/94	0.025	0.013	ZI
MES B3 NW NST	6/09/94	0.035	0.000	ZI

¹ Normalized sum of residuals squared.

² Normalized runoff volume.

W wheel traffic compaction.

NW non-wheel traffic.

ST strawed furrows.

NST non-strawed furrows.

ZI zero-inertia solution.

KW kinematic-wave solution.

For most irrigation simulations in Table 6.8, the zero-inertia solution was chosen. The zero-inertia solution was found to be most appropriate for high intake conditions (non-wheel compacted furrows) and for fields with shallow slopes. In general, additional computational time was required for the zero-

inertia solutions versus the kinematic wave, but the simulation was less likely to fail during execution, especially for conditions of highly non-linear intake. The kinematic wave solution worked well with the steeply sloped, wheel traffic compacted furrows of Field B3 at the Malheur Experiment Station (June 1, 1994). Under these conditions, a uniform depth of flow is quickly achieved by the irrigation stream.

A compilation is given of field observation and simulation results in Tables 6.9 and 6.10. Table 6.9 shows the total inflow and runoff volumes and Table 6.10 shows the corresponding percentage of infiltration and runoff.

Table 6.9 Inflow and runoff data from all observed irrigation events. Field data are compared with SRFR simulation results

Farm ID	Date	Field observed		SRFR results	
		Infl. m ³	Runoff m ³	Infl. m ³	Runoff m ³
MES B7 W	5/11/93	37.1	12.9	37.1	12.2
MES B7 NW	5/11/93	37.5	0.1	37.4	0.1
MES B7 W	6/14/93	34.2	9.5	34.2	7.8
MES B7 NW	6/14/93	35.1	4.6	35.1	2.5
Bel-Air W	4/12/94	44.8	5.8	44.8	5.3
Bel-Air NW	4/12/94	46.8	0.0	46.8	0.0
Duyn W	9/03/93	52.7	17.1	52.7	17.2
Duyn NW	9/03/93	57.5	0.6	57.5	1.0
Cruick. NW	7/22/93	46.7	2.4	46.7	2.3
MES B3 W ST	6/01/94	14.2	10.0	14.2	10.3
MES B3 W NST	6/01/94	15.0	12.1	15.0	12.2
MES B3 NW ST	6/09/94	15.1	0.9	15.2	0.7
MES B3 NW NST	6/09/94	14.8	4.4	14.9	4.4

Table 6.10 Percent infiltration and runoff from all observed irrigation events. Field data are compared with SRFr simulation results.

Farm ID	Date	Field observed		SRFR results	
		Infil. %	Runoff %	Infil. %	Runoff %
MES B7 W	5/11/93	65.2	34.8	67.1	32.9
MES B7 NW	5/11/93	99.7	0.3	99.6	0.4
MES B7 W	6/14/93	72.4	27.6	77.2	22.8
MES B7 NW	6/14/93	87.0	13.0	92.9	7.1
Bel-Air W	4/12/94	87.2	12.8	88.2	11.8
Bel-Air NW	4/12/94	100.	0.0	100.	0.0
Duyn W	9/03/93	67.6	32.4	67.3	32.7
Duyn NW	9/03/93	99.0	1.0	76.9	23.1
Cruick. NW	7/22/93	94.8	5.2	95.0	5.0
MES B3 W ST	6/01/94	29.3	70.7	27.7	72.3
MES B3 W NST	6/01/94	19.4	80.6	18.8	81.2
MES B3 NW ST	6/09/94	94.1	5.9	95.2	4.8
MES B3 NW NST	6/09/94	70.5	29.5	70.7	29.3

Following are several figures showing the results of model calibration of individual irrigation events with field data. For the examples, a field of medium length and shallow field slope (MES Field B7) was chosen along with a long field of variable slope (Bel-Air Farms) and finally a short, steeply sloped field (MES Field B3).

Wheel traffic and non-wheel traffic furrow advance times for the first irrigation of Field B7 at the Malheur Experiment Station on May 11, 1993 are shown in Figure 6.11. The field slope, which is also shown in Figure 6.11, averages 0.55 percent and is relatively uniform. The stream in the non-wheel traffic furrow completed advance just after 1200 minutes. The wheel traffic furrow reached the end of the field in only 175 minutes. By inspection of the advance rates, it can be seen that intake in the non-wheel traffic furrow is greater. Model simulation advance rates follow field observed advance rates closely with no large discrepancies, although for the non-wheel traffic furrow, the shape of the advance curves differ somewhat. Field data show a slightly more rapid advance early in the irrigation.

Water distribution from the first irrigation of Field B7 are shown in Figures 6.12 and 6.13 for the non-wheel and wheel traffic furrows respectively. Both figures show a relatively even water distribution along the field although the advance time for the non-wheel traffic furrow was over 1200 minutes.

Soil moisture data for the non-wheel traffic furrow indicate an 11.6 cm (4.6 in) mean infiltration depth while flow measurements result in a 12.6 cm (5.0 in) mean infiltration depth. Soil moisture in the 1.8 meter (6 ft) profile was uniformly high along the non-wheel traffic furrow (mean of 0.31 cm cm^{-1} with an estimated field capacity of 0.36 cm cm^{-1}) prior to this first irrigation. It is possible that water infiltrated below the 1.8 m access tube depth or was forced laterally since only 9.1 cm (3.6 in) of water could be held within the top 1.8 m (6 ft) of the soil profile based on the mean initial soil moisture. This would

indicate that the change in soil moisture at the top of the field could not fully account for the infiltrated depth (see Figure 6.12). It is also possible that actual field capacity was significantly different from the nominal 0.36. The SRFR simulation indicated that nearly 20 cm of water (7.9 in) infiltrated the soil near the top of the field and less than 4 cm (1.6 in) at the bottom of the field.

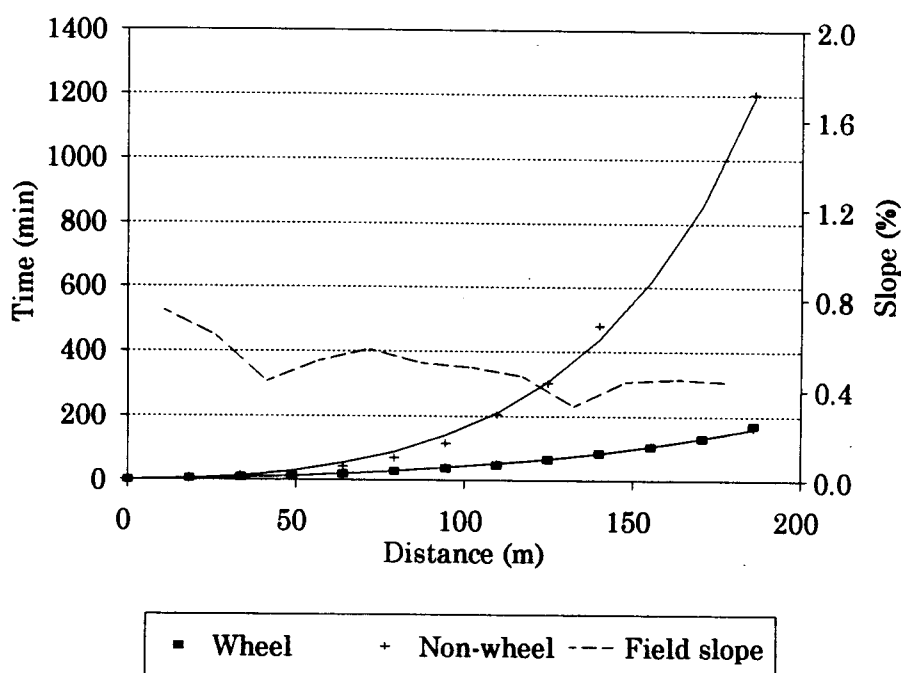


Figure 6.11 Field observed and SRFR advance times of non-wheel and wheel traffic compacted furrows for the May 11, 1993 irrigation of Field B7 at the O.S.U. Malheur Experiment Station, Ontario, Oregon, 1993.

Figure 6.13 shows the results from the wheel traffic compacted furrow. Interestingly, neutron probe soil moisture data show an even distribution with slightly greater infiltration on the bottom half of the field in comparison to the distribution derived from measured furrow flows. Mean soil moisture prior to

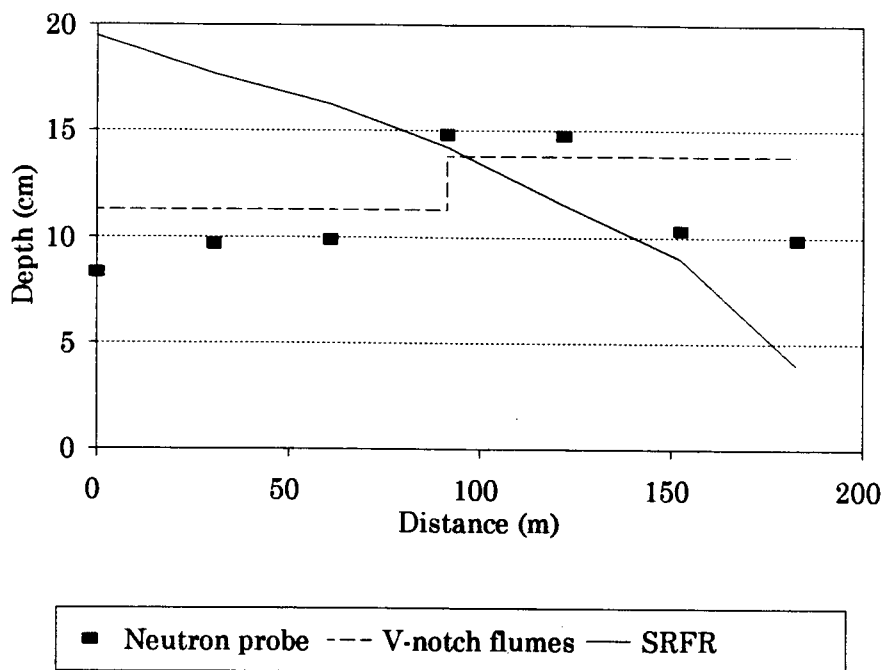


Figure 6.12 Distribution of infiltrated water on non-wheel traffic compacted furrow, May 11, 1993, Field B7, O.S.U. Malheur Experiment Station, Ontario, Oregon.

the irrigation was 0.30 which allowed for approximately 11 cm of additional storage in the top 1.8 m (6 ft). SFRF predicts an infiltrated depth of nearly 9.0 cm (3.5 in) at the top of the field. Neutron probe measurements indicate that the average depth infiltrated was 11.0 cm (4.3 in) and flow measurements indicate an 8.2 cm (3.2 in) average depth of infiltration. The difference may be partly due to flow measurement error, but is likely attributable to variations in intake along the furrow and interference from adjacent irrigated furrows.

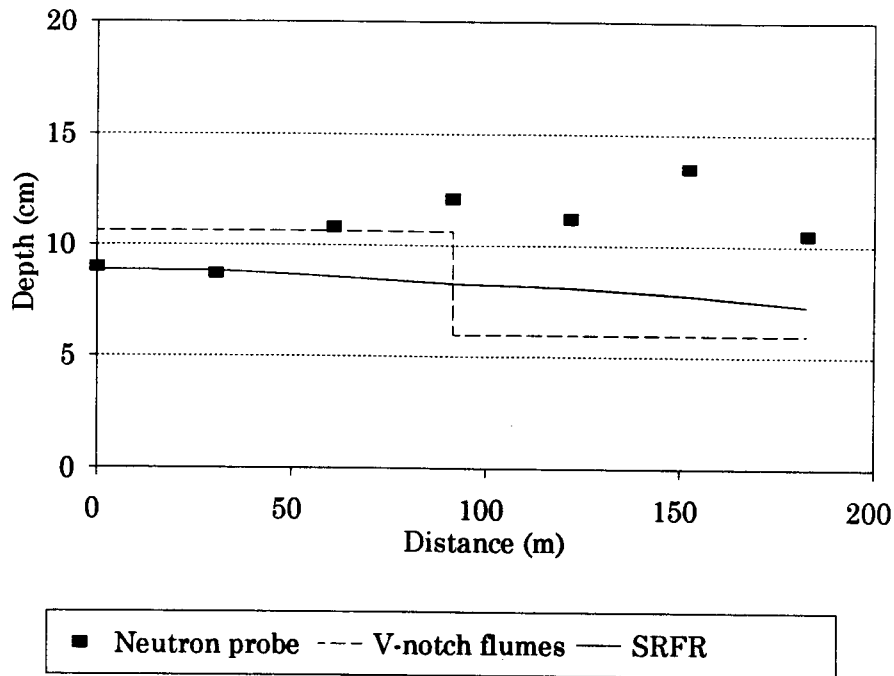


Figure 6.13 Distribution of infiltrated water on wheel traffic compacted furrow, May 11, 1993, Field B7, O.S.U. Malheur Experiment Station, Ontario, Oregon.

The water distributions simulated by SRFR did not compare well with field data. The distribution uniformity, DU_{LQ} , predicted by SRFR was 0.49 and 0.91 respectively for non-wheel and wheel traffic furrows. From neutron probe measurements, the DU_{LQ} values were estimated to be a much more uniform 0.87 and 1.09 respectively. Finally, estimates from furrow flow measurements indicate contrasting DU_{LQ} values close to 1.10 and 0.72 respectively. From these data it appears that one or more of the following are true: 1) initial conditions in the field are not uniform (non-uniform intake); 2) interference from adjacent furrows has affected soil moisture readings; 3) the placement of neutron probe

access tubes did not sufficiently measure the change in soil moisture; or 4) measurement error is much larger than anticipated.

The Bel-Air Farms winter wheat crop in 1994 followed a rotation in alfalfa leaving this silt loam soil with improved structure (a measured bulk density of 1.0 g cc^{-1}) and greater permeability. Though the average slope was near 0.8 percent, the slope varied, increasing in general, from the top to the bottom (as seen in Figure 6.14). This early in the season, crop vegetation was not important in contributing to the hydraulic roughness of the furrow. Predictably, a difference in irrigation advance times is evident between wheel and non-wheel traffic furrows (Figure 6.15). The stream in the non-wheel furrow only reached midfield by the end of the irrigation.

Figures 6.15 and 6.16 show the corresponding water distributions from the non-wheel and wheel traffic furrows. Soil moisture prior to the irrigation averaged 0.30 in the top 90 cm (36 in) of the soil profile. The average infiltration depth was measured from flow data to be 16.3 cm (6.4 in) for the non-wheel furrow and 13.6 cm (5.3 in) for the wheel traffic furrow. Distribution uniformity, DU_{LQ} , as predicted by the SFRF model was 0.01 for the non-wheel furrow (because the stream did not advance the length of the field) and 0.65 for the wheel traffic furrow. From flume measurements, DU_{LQ} was calculated to be 0.23 and 0.80 respectively. It appears that intake varied along the furrow judging by the irregular distribution of furrow flow observed in both non-wheel

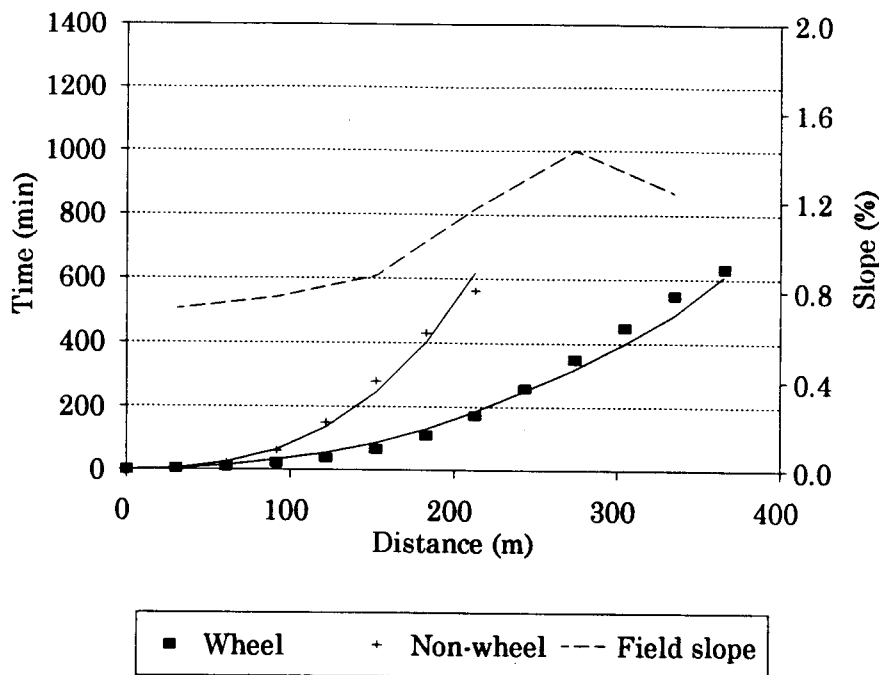


Figure 6.14 Field observed and SRFR simulation stream advance times for non-wheel and wheel traffic furrows from the April 12, 1994 irrigation of winter wheat at Bel-Air Farms.

and wheel traffic furrows. It is possible that soil physical properties varied along the field due to factors determined by field history and the local geology.

An extremely high infiltration depth of over 40 cm (15.7 in) was predicted by the SRFR model for the top of the non-wheel furrow though the measured infiltration depth was nearer to 22 cm (8.6 in). This difference may be due to an overestimation of the long term intake rate, as determined by the intake coefficient b , in the SRFR simulation. No runoff occurred for this furrow for SRFR calibration and so the simulation was calibrated solely with advance data.

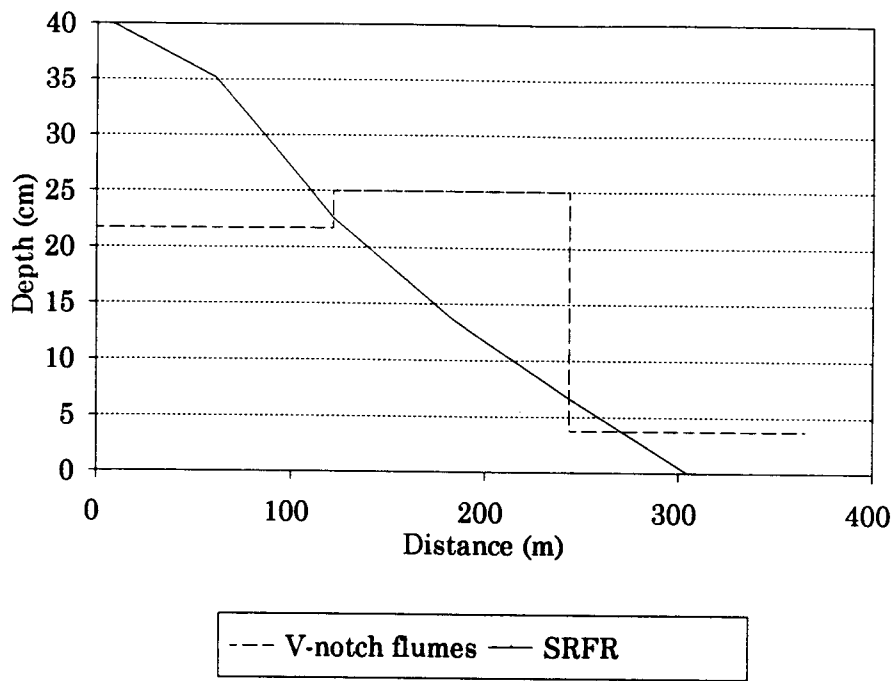


Figure 6.15 Distribution of infiltrated water for a non-wheel traffic furrow, April 12, 1994, Bel-Air Farms.

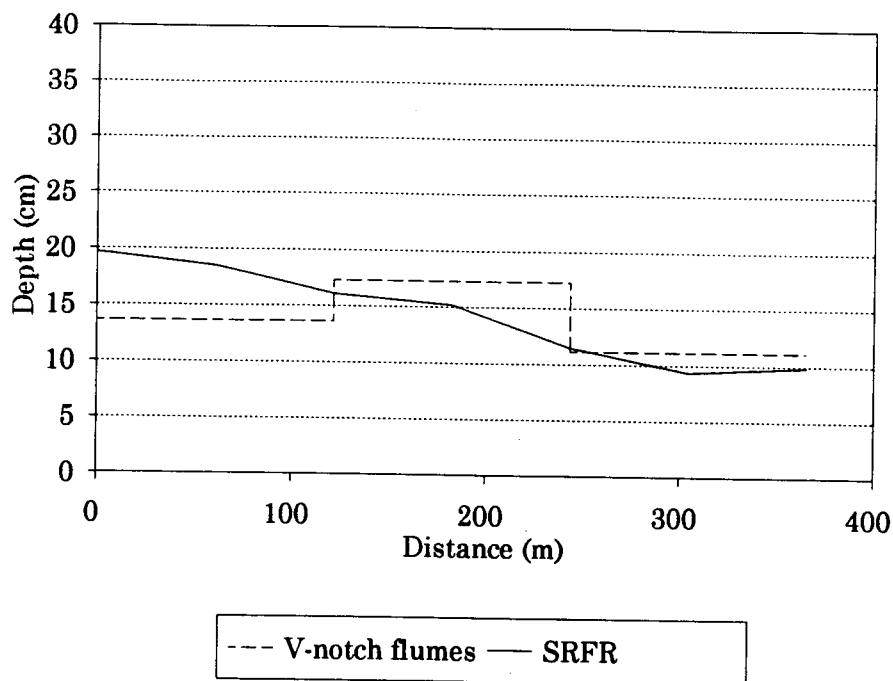


Figure 6.16 Distribution of infiltrated water on wheel traffic compacted furrow, April 12, 1994, Bel-Air Farm.

Advance times for the June 1, 1994 irrigation of Field B3 potatoes at the Malheur Experiment Station are shown in Figure 6.17. For this irrigation of wheel traffic compacted furrows, advance rates were rapid. Advance in strawed furrows was at approximately one half the rate of non-strawed furrows.

Very little water infiltrated for both straw and non-strawed furrows irrigated on June 1, as can be seen in Figures 6.18 and 6.19. Mean initial soil moisture prior to irrigation for this silt loam was measured to be 0.27 cm cm^{-1} in the non-strawed furrow and 0.26 cm cm^{-1} in the strawed furrow, to a depth of 1.8 m (6 ft). Based on a field capacity of 0.36, approximately 17 cm of storage

were available in the top 183 cm. Even so, runoff percentages were extremely high at approximately 80 percent (Table 6.10). Due to the rapid stream advance, the uniformity of the irrigation should have been high. From neutron probe soil moisture data a DU_{LQ} of 0.61 and 0.72 was calculated for the strawed furrow and bare furrow respectively. SRFR predicted a greater DU_{LQ} of 0.92 and 0.94 respectively.

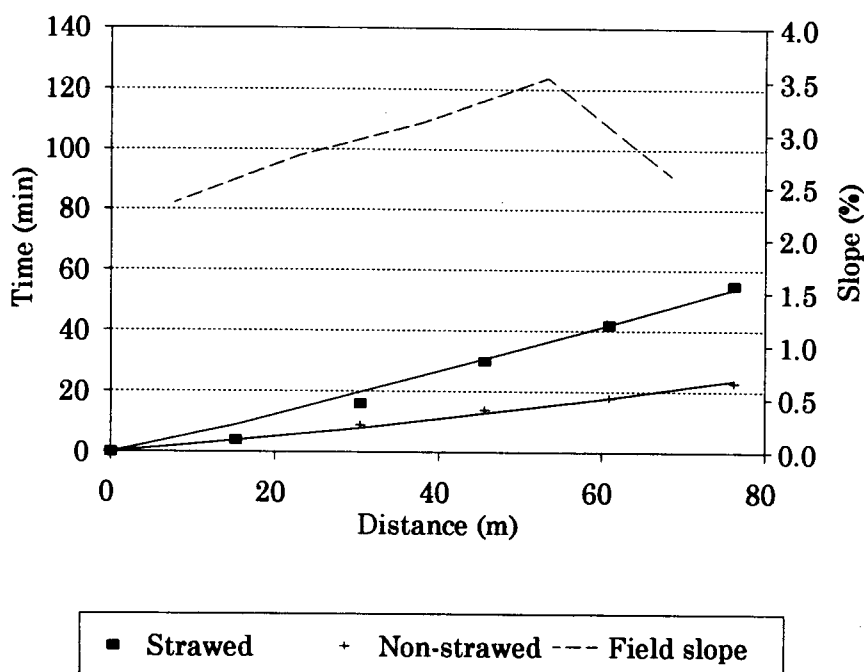


Figure 6.17 Advance rates for the June 1, 1994 irrigation of potatoes on Field B3 at the O.S.U. Malheur Experiment Station.

A slightly greater application depth was measured in the strawed furrow resulting from an increase in stream wetted perimeter compared to bare soil conditions. Neutron probe measurements showed a mean application depth of

4.5 cm (1.8 in) for the strawed furrow and 1.5 cm (0.6 in) for the non-strawed furrow. Flow measurements indicate a mean infiltrated depth of 3.3 cm (1.3 in) in the strawed furrow and 2.4 cm (0.9 in) in the non-strawed furrow. Though these data have not been tested by a statistical analysis, research conducted by Shock et al. (1994) concluded a significant increase in infiltration of strawed furrows over non-strawed furrows. The importance of straw mulching to furrow hydraulics cannot be neglected.

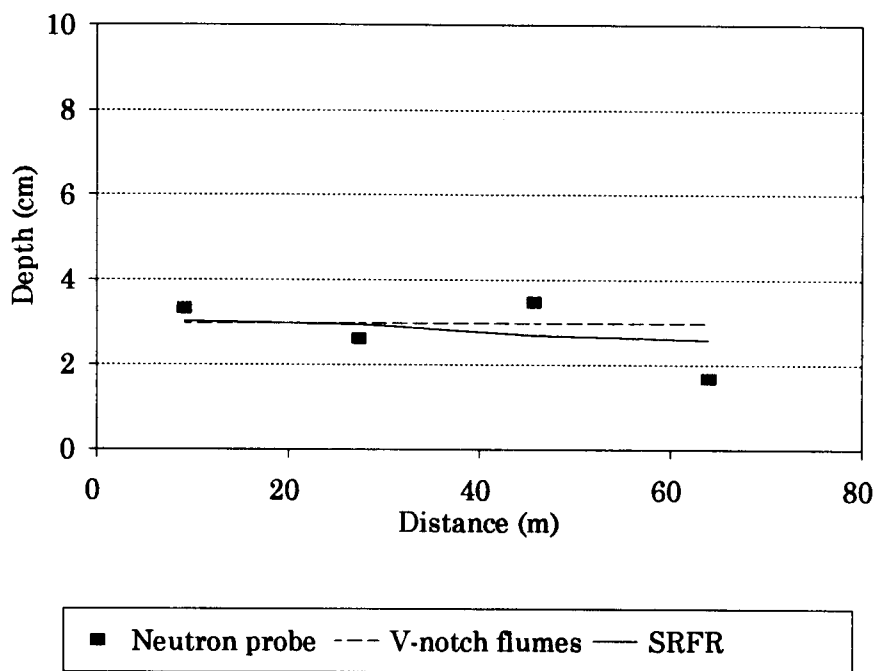


Figure 6.18 Distribution of infiltrated water along a wheel traffic compacted, strawed furrow, June 1, 1994, Field B3, O.S.U. Malheur Experiment Station.

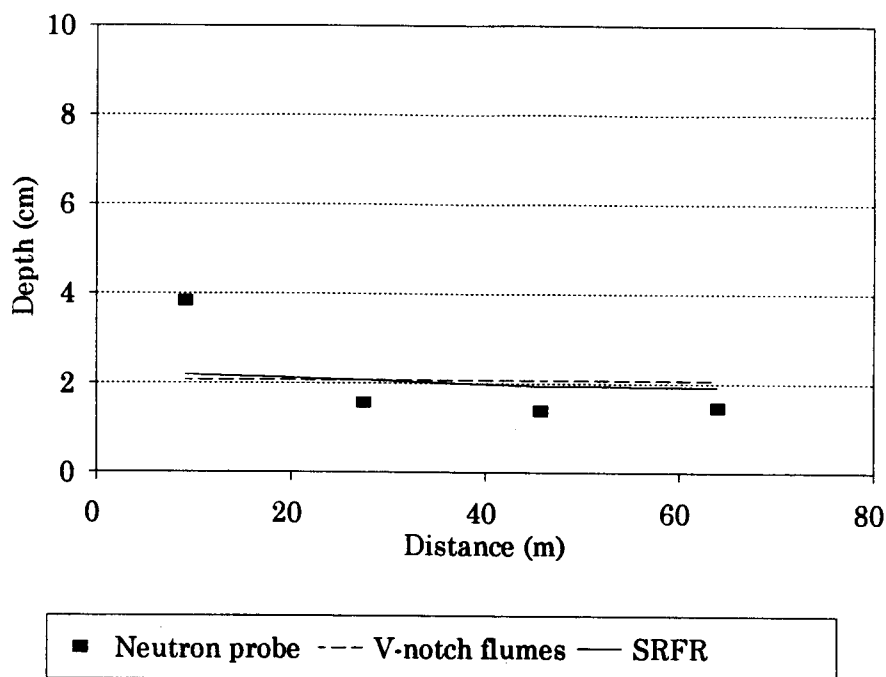


Figure 6.19 Distribution of infiltrated water along a wheel traffic compacted, non-strawed furrow, June 1, 1994, Field B3, O.S.U. Malheur Experiment Station.

The first irrigation of non-wheel traffic furrows was on June 9, 1994. Streams in both strawed and non-strawed furrows advanced more slowly than during the June 1 irrigation, especially in the strawed furrow (Figure 6.20).

The water distribution from the June 9, 1994 irrigation (Figures 6.21, and 6.22) contrast with the June 1, 1994 irrigation. Antecedent soil moisture was high for this irrigation at 0.28 cm cm^{-1} for the non-strawed furrow and 0.30 cm cm^{-1} for the strawed furrow (measured to 180 cm). Infiltrated depths averaged 10.2 cm (4.0 in) for the strawed furrow and 7.5 cm (3.0 in) for the non-strawed furrow from flow measurements. Neutron probe soil moisture data

showed the average infiltrated depth to be 8.0 cm (3.1 in) in the strawed furrows and 7.9 cm (3.1 in) in non-strawed furrows. It can be seen in Figures 6.21 and 6.22 that the infiltrated depth decreases down the furrow corresponding to differences in intake opportunity time. Distribution uniformities, DU_{LQ} , calculated from neutron probe data are 0.57 and 0.76 for the strawed and non-strawed furrows respectively. SRFr predicted similar respective DU_{LQ} values of 0.62 and 0.85.

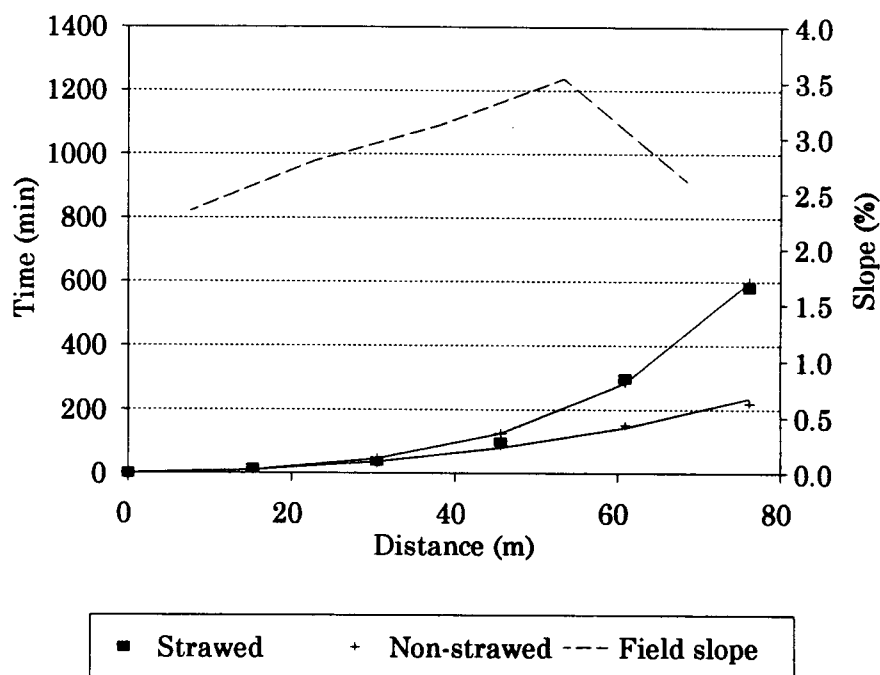


Figure 6.20 Field observed and SRFr simulation stream advance times from the June 9, 1994 irrigation of potatoes planted on Field B3 at the O.S.U. Malheur Experiment Station.

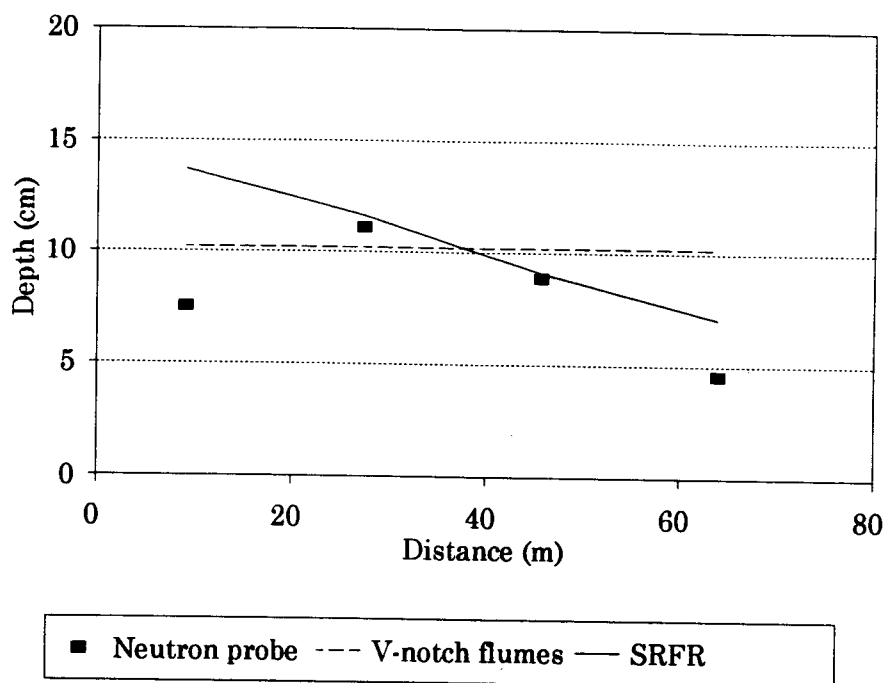


Figure 6.21 Distribution of infiltrated water along a non-wheel traffic compacted, strawed furrow, June 9, 1994, Field B3, O.S.U. Malheur Experiment Station.

The spacing of potato furrows at 91 centimeters (36 in), coupled with an alternating furrow irrigation strategy, created a situation where lateral wetting was incomplete. Neutron probe access tubes were placed in the center of the crop bed approximately 46 cm (18 in) away from the center of the irrigation stream, so it is possible that the position of the access tubes about the irrigated furrow did not allow for a sufficient measure of the average change in soil moisture, though ET loss between measurement periods was accounted for.

From this exercise, several observations are made. The change in soil moisture along the furrow, as measured with the neutron probe, does not

necessarily reflect irrigation performance as predicted by the SRFR model. Differences in intake may be attributed to variation in compaction and soil moisture. Also, neutron probe measurements only provide data for a point location in the field and cannot fully account for the heterogeneity of lateral and vertical soil water movement. Furrow v-notch flume measurements, when used consistently, provide the most reliable method for measuring water distribution along long sections of the furrow. In SRFR, the assumption of uniform intake characteristics along the furrow (unless otherwise specified) does not allow for a precise prediction of water distribution in a soil of heterogeneous properties.

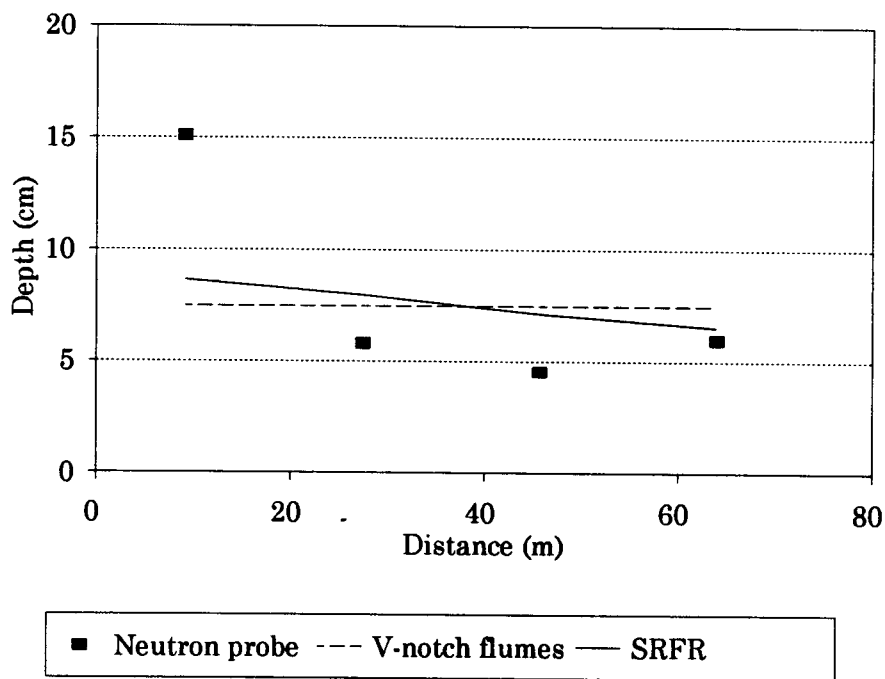


Figure 6.22 Distribution of infiltrated water along a non-wheel traffic compacted, non-strawed furrow, June 9, 1994, Field B3, O.S.U. Malheur Experiment Station.

6.5 Seasonal variation in irrigation performance

Optimization of furrow irrigation performance is difficult due to the seasonal variation of intake characteristics and furrow conditions. If these variations are neglected, overall irrigation efficiencies will be lower than necessary. Many growers recognize this and adjust siphon tube levels or gated pipe openings and irrigation set times as the season progresses. When using hydraulic irrigation models for the purpose of evaluating "best management practices", seasonal variations must be recognized in field characteristics, and in particular, furrow intake.

The five irrigations of Field B7 during 1993 were monitored for inflow and outflow on both wheel traffic compacted and non-wheel furrows. Irrigations were on alternating furrows. The irrigation dates were May 11, June 14, July 1, July 14, and July 29 of 1993 and the original set times for each irrigation were 26, 28, 24, 24 and 24.5 hours. Results from each irrigation were truncated to represent 24 hour set times so that runoff data are comparable (Figure 6.23 and Table 6.11). Furrow inflow rates for the season ranged between 0.30 to 0.40 l s^{-1} (5 to 6 gpm). PVC gated pipe with valves at each outlet was used to distribute the water at the head of each furrow and a weed screen with an overflow spillway was used to maintain a constant head.

For wheel traffic furrows, there was less infiltration and runoff was high due to the lower intake rate of compacted furrows (Figure 6.23). The percent runoff generally increased for each irrigation to a maximum of 46.3% for the

fourth irrigation. The average percent runoff for each irrigation was 30.8%.

For all non-wheel traffic furrow irrigations, infiltration was greater and runoff less than for wheel traffic furrows. But because of the consolidation of the soil in the irrigated furrow bed and resulting decrease in permeability, runoff became important during the fourth and fifth irrigations at 24.3% and 18.0% respectively. The average percent runoff for each irrigation was 9.6%. A more complete analysis from these same irrigation evaluations, including surge irrigation results, is presented by Shock et al. (1994).

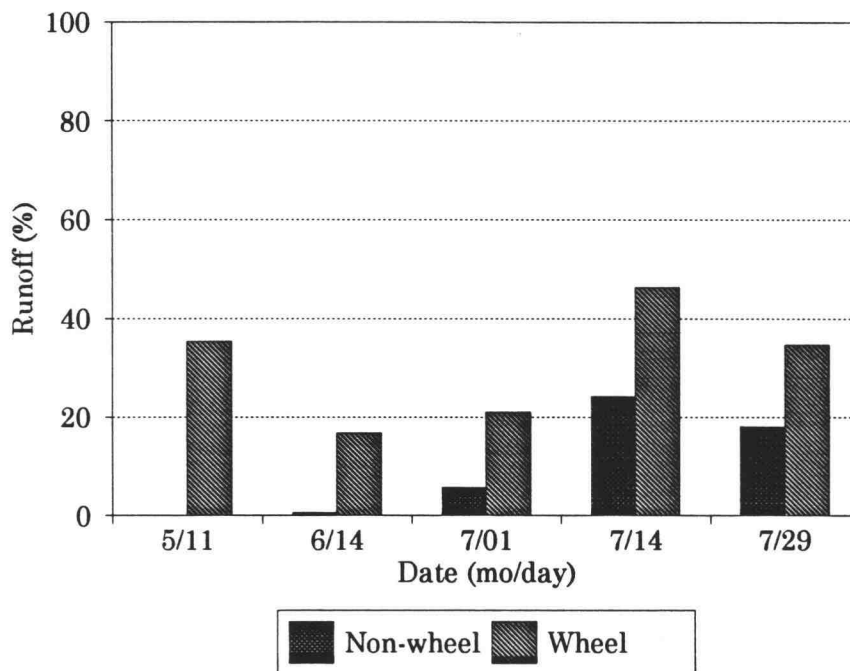


Figure 6.23 Percent runoff for each irrigation of Field B7 during 1993 at the Malheur Experiment Station. Results are from both non-wheel traffic and wheel traffic furrows.

Table 6.11 Field B7 runoff percentages from each irrigation, 1993

Date	Inflow m ³	Runoff m ³	Runoff %	θ_i cm cm ⁻¹	Z _{req} cm
Non-wheel					
May 11	34.6	0.0	0.00	0.31	10
June 14	29.8	1.2	4.00	0.35	6
July 1	28.2	1.6	5.70	0.33	7
July 14	32.5	7.9	24.3	0.39*	6
July 29	31.6	5.7	18.0	0.34	6
Wheel					
May 11	34.2	12.1	35.4	0.33	10
June 14	29.1	4.9	16.8	0.33	6
July 1	28.1	5.9	21.0	0.32	7
July 14	32	14.8	46.3	0.36*	6
July 29	31.2	10.8	34.6	0.33	6

*Neutron probe readings may not have been reliable on this date.

7. SUMMARY

Row crops in Northeast Malheur County are typically furrow irrigated by continuous flow methods using gated pipe or siphon tubes. Inflow rates chosen by irrigators range from 0.10 l s^{-1} to 0.7 l s^{-1} (2 to 11 gpm) depending on field slope and tractor wheel traffic compaction. No typical field length exists, but fields are rarely longer than 390 m (1280 ft) or shorter than 30 m (100 ft). Many fields are one quarter mile in length (390 m). Area wide, most field slopes are less than 1.5 percent, though some irrigated fields do have slopes that exceed 3 percent. Observed irrigation set times (durations) were most frequently 12 or 24 hour sets for the convenience of the irrigation.

Furrow intake characteristics vary greatly depending on several factors which include wheel traffic compaction, initial soil moisture, and crop development. Presumably, soil texture is also important but too few infiltration tests were conducted on soils other than silt loams to draw definite conclusions. Tractor wheel traffic proved to be the greatest factor in determining intake characteristics. Long term intake rates in non-wheel traffic furrows averaged $5.6 \text{ l m}^{-1}\text{h}^{-1}$ and wheel traffic furrows averaged $2.8 \text{ l m}^{-1}\text{h}^{-1}$. Using the Extended Kostiakov equation, two intake curves were derived from inflow-outflow data to represent intake in wheel traffic and non-wheel traffic furrows (Table 6.1). For use in SRFR, the Extended-Kostiakov coefficients must be normalized by dividing by the mean wetted perimeter, which may be found by estimating the

section factor, F (equation 12), and using the power curve relationship derived in Section 6.2. The mean wetted perimeter may also be determined from field measurements.

The hydraulic roughness, represented by Manning's n , ranged from 0.035 to 0.12 for bare soil conditions free of vegetation. Crop vegetation contributed significantly to hydraulic roughness late in the growing season. This was especially important in potato and sugar beet fields where vegetation collapsed into the furrows. In one sugar beet field, Manning's n was calculated to average 0.12 late in the growing season. Straw mulching also greatly increased hydraulic roughness. Calculations for straw mulched furrows showed Manning's n to range from 0.15 to 0.36 with an average of 0.27. Recommended Manning's n values are given in Table 6.3 for various field conditions.

Furrow size and shape initially depend on the size of the shovel attached to the drawbar for cultivation. Furrow shape is also dependent upon the number irrigations following cultivation. For field slopes of less than 0.5 percent, late in the season after layby (when tractor traffic is no longer possible) furrows tend to become increasingly shallow and wider as the stream erodes the sides of the channel and as sediment settles in the furrow bed. For field slopes greater than 1.5 percent channel bed erosion becomes increasingly important (Tunio, 1994). To model the furrow shape, a trapezoid, with varying bed width, b , and side-slope, z , was assumed to represent furrow channel shape. In general, furrow dimensions presented within this thesis are valid for slopes of

less than 1.5 percent where erosion due to the scouring of the channel bed is not excessive.

The fiberglass flumes proved to be the most valuable tool in irrigation analysis. These were used to measure both irrigation water distribution along the furrow and furrow intake characteristics. Installation of these flumes requires considerable care so that water is not ponded upstream of the flume, and so that a hydraulic "jump" may be continuously observed at the throat constriction. Proper installation was obtained by eliminating bypass flow and by leveling the flume in both longitudinal and lateral directions. Flumes were difficult to use with wide furrows, such as those used in potato fields, or on excessively steep fields ($>3\%$) and also on very shallow fields ($<0.50\%$) because water would pond upstream of the flume.

In furrow irrigation systems, a tremendous number of variables are involved, both in management practices and in physical conditions. Furthermore, furrow irrigation processes are largely transient, reaching "steady-state" conditions late in the irrigation. Ideally, a larger number of irrigation evaluations should have been conducted to broaden the data base from which conclusions were drawn. Of particular importance are the measured intake curves for various soil types and field conditions. Though furrow intake can vary greatly for similar conditions, additional data may allow the separation of intake curves into more distinct families based on initial soil moisture, furrow condition and soil texture. Furrow cross-section measurements from a greater number of fields and furrow conditions would be also invaluable. This would

allow a greater association of furrow shape with such factors as field slope, shovel size, crop type and degree of compaction.

Of value to the development of the SRFR model would be the calibration of SRFR for surge irrigation. Surge irrigation trials conducted at the Malheur Experiment Station (Shock et al., 1994) have shown promising results and have attracted the attention of many growers.

The SRFR hydraulic irrigation model, developed by the U.S. Water Conservation Lab, was calibrated for individual irrigation events with field data obtained from several farm sites in northeastern Malheur County, Oregon. Once calibrated, the SRFR hydraulic irrigation model may be used as a predictive tool, able to evaluate the performance of various irrigation options including, but not limited to, flow cut-back, surge flow, alternate furrow irrigation and field laser-leveling. Because of the variable nature of furrow systems, SRFR will not necessarily be able to predict the performance of individual irrigation events though calibration with field data for individual events will provide a basis for predicting changes in irrigation performance for changes in operational practices.

BIBLIOGRAPHY

- American Society of Agricultural Engineers. 1983. Advances in infiltration. Proceedings of the National Conference on Advances in Infiltration, December 12-13, 1983, Chicago, IL., pages 240-248.
- American Society of Civil Engineers/ASCE. 1978. Describing irrigation efficiency and uniformity. By the on-farm irrigation committee of the Irrigation and Drainage Division of the ASCE. Proceedings of the ASCE 104, IRI: 35-41.
- Anon. 1978. Water conservation opportunities study. U.S. Dept. Of Interior, Bureau of Reclamation and Bureau of Indian Affairs, Washington, D.C.
- Bali, K., Wallender, W.W. 1987. Water application under varying soil and intake opportunity time. Trans. ASAE, Vol. 30, No. 2, pages 442-448.
- Barnum, J.M., Feibert, E.B.G., Shock, C.C. 1995. 1994 Weather Report. Oregon State University Agricultural Experiment Station Special Report 947, p. 229-244.
- Bautista, E., Wallender, W.W.I 1993. Numerical calculation of infiltration in furrow irrigation simulation models. J. of Irrigation and Drainage Engineering, Vol. 119, No. 2, pages 286-311.
- Bautista, E., Wallender, W.W.I 1993. Reliability of optimized furrow-infiltration parameters. J. of Irrigation and Drainage Engineering, Vol. 119, No. 5, pages 784-799.
- Blair, A.W., Smerdon, E.T. 1988. Infiltration from irrigation advance data. II: Experimental. J. of Irrigation and Drainage Engineering, Vol. 114, No. 1, February, 1988, p. 4.
- Blair, A.W., Trout, T.L. 1989. Recirculating furrow infiltrometer design guide. Technical Report CRWR 223. Center for Research in Water Resources, University of Texas, Austin.
- Brown, M.J., Kemper, W.D., Trout, T.J., Humpherys, A.S. 1988. Sediment, erosion and water intake in furrows. Irrigation Science, Vol. 9, pages 45-55.
- Childs, J.L., Wallender, W.W.I, Hopmans, J.W. 1993. Spatial and seasonal variation of furrow infiltration. J. of Irrigation and Drainage Engineering, Vol. 119, No. 1, pages 74-90.

- Chow, V.T. 1959. Open channel hydraulics. McGraw-Hill, Inc., New York, N.Y.
- Davis, J.R., Fry, A.W. 1963. Measurement of infiltration rates in irrigated furrows. *Trans. ASAE*, Vol. 6, No. 4, pages 318-319.
- Eldredge, E.P., Shock, C.C., Stieber, T.D. 1993. Calibration of granular matrix sensors for irrigation management. *Agronomy Journal*, Vol. 85, No. 6, pages 1228-1232.
- Elliott, R.L., Walker, W.R. 1982a. Field evaluation of furrow infiltration and advance functions. *Trans. ASAE*, Vol. 25, No. 2, pages 396-400.
- Elliott, R.L., Walker, W.R., Skogerboe, G.V. 1982b. Zero-inertia modeling of furrow irrigation advance. *J. Of Irrigation and Drainage Engineering*, Vol. 108, p. 179-195.
- Elliott, R.L., Walker, W.R., Skogerboe, G.V. 1983a. Furrow irrigation advance rates: A dimensionless approach. *Trans. ASAE*, Vol. 26, No. 6, 1983, p. 1722.
- Elliott, R.L., Walker, W.R., Skogerboe, G.V. 1983b. Infiltration parameters from furrow irrigation advance data. *Trans. ASAE*, Vol. 26, No. 6, 1983, p. 1726.
- Erie, L.J. 1962. Evaluation of infiltration measurements. *Trans. ASAE*, Vol. 5, No. 1, pages 11-13.
- Fangmeier, D.D., Ramsey, M.K. 1978. Intake characteristics of irrigation furrows. *Trans. ASAE*, Vol. 21, No. 4, pages 696-700.
- Hill, R.L. 1993. Tillage and wheel traffic effects on runoff and sediment losses from crop interrows. *Soil Science Society of America J.*, Vol. 57, pages 476-480.
- Izadi, B., Studer, D., McCann, I. 1991. Maximizing set-wide furrow irrigation application efficiency under full irrigation strategy. *Trans. ASAE*, Vol. 34, No. 5, page 2006.
- Kemper, W.D., Ruffing, B.J., Bondurant, J.A. 1982. Furrow intake rates and water management. *Trans. ASAE*, Vol. 25, pages 333-343.
- Kincaid, D.C. 1986. Intake rate: Border and furrow. p. 871. In A. Klute (ed.) *Methods of soil analysis. Part 1*, 2nd ed. Agron. Monogr. 9. ASA, Madison, WI.

- Koluvek, P.K., Tanji, K.K., Trout, T.J. 1993. Overview of soil erosion from irrigation. *J. of Irrigation and Drainage Engineering*, Vol. 119, No. 6, pages 929-963.
- Lentz, R.D., Shainberg, I., Sojka, R.E., Carter, D.L. 1992. Preventing irrigation furrow erosion with small applications of polymers. *Soil Science Society of America Journal*, Vol. 56, 1992, p. 1926.
- Lewis, M.R., Milne, W.E. 1938. Analysis of border irrigation. *Agricultural Engineering*, Vol. 19, No. 6, p. 267.
- Ley, T.W. 1978. Sensitivity of furrow irrigation performance to field and operation variables. M.S. thesis presented to Colorado State University, at Ft. Collins.
- Linderman, C.L., Stegman, E.C. 1971. Seasonal variation of hydraulic parameters and their influence upon surface irrigation application efficiency. *Trans. ASAE*, Vol. 14, 1971, p. 914.
- Merriam, J.L. 1988. Drouth problems mitigated by controlled irrigation frequency with flexible water delivery schedule. USCID Meeting, September 14-16, 1988, San Diego, California.
- Mitchell, A.R., van Genuchten, M.Th. 1993. Flood irrigation of a cracked soil. *Soil Science Society of America J.*, Vol. 57, pages 490-497.
- Oliveira, C.A.S., Hanks, R.J., Shani, U. 1987. Infiltration and runoff as affected by pitting, mulching and sprinkler irrigation. *Irrigation Science*, Vol. 8, pages 49-64.
- Oweis, T.Y., Walker, W.R. 1990. Zero-inertia model for surge flow furrow irrigation. *Irrigation Science*, Vol. 11, pages 131-136.
- Richards, L.S. 1931. Capillary conduction through porous media. *Physics*, Vol. 1, pages 318-333.
- Robinson, A.R., Chamberlain, A.R. 1960. Trapezoidal flumes for open channel flow measurement. *Trans. ASAE*, Vol. 13, No. 2, pages 120-128.
- Samani, Z.A., Walker, W.R., Jeppson, R.W., Willardson, L.S. 1985. Numerical Solution for unsteady two-dimensional infiltration in irrigation furrows. *Trans. ASAE*, Vol. 28, No. 4, pages 1186-1190.

- Schwankl, L.J., Wallender, W.W.I 1988. Zero-inertia furrow modeling with variable infiltration and hydraulic characteristics. *Trans. ASAE*, Vol. 31, No. 5, pages 1470-1475.
- SCS/USDA. 1984. National engineering handbook, section 15, irrigation, chapter 5, furrow irrigation.
- SCS/USDA. 1981. Soil Survey of Northeast Malheur County.
- Segeren, A.G., Trout, T. 1991. Hydraulic resistance of soil surface seals in irrigated furrows. *Soil Science Society of America J.*, Vol. 55, pages 640-646.
- Shock, C.C., Saunders, L.D., Shock, B.M., Hobson, J.H., English, M.J., Mittelstadt, R.W. 1994. Improved irrigation efficiency and reduction in sediment loss by mechanical furrow mulching wheat. Oregon State University Agricultural Experiment Station Special Report 936, pages 187-190.
- Shock, C.C., Zattiero, J., Kantola, K., Saunders, L.D. 1995. Comparative cost and effectiveness of polyacrylamide and straw mulch or sediment loss from furrow irrigated potatoes. Oregon State University Agricultural Experiment Station Special Report 947, pages 128-137.
- Smerdon, E.T., Blair, A.W., Reddell, D.L. 1988. Infiltration from irrigation advance data. I: Theory. *J. of Irrigation and Drainage Engineering*, Vol. 114, No. 1, February, 1988, p. 4.
- Sojka, R.E. 1994. Polyacrylamide (PAM). Unpublished technical paper. USDA-ARS, Soil and Water Management Research Unit, Kimberly, Idaho.
- Strelkoff, T.S. 1984. Modeling effect of depth on furrow infiltration. *J. of Irrigation and Drainage Engineering*, Vol. 110, No. 4, pages 375-387.
- Strelkoff, T.S. 1985. Dimensionless formulation of furrow irrigation. *J. of Irrigation and Drainage Engineering*, Vol. 111, No. 4, pages 380-395.
- Strelkoff, T.S. 1990. SRFR: A computer program for simulating flow in surface irrigation, WCL Report #17, U.S. Water Conservation Laboratory, USDA/ARS, December, 1990.
- Strelkoff, T.S. 1992. Computer simulations and SCS furrow design. Paper presented at 1992 ASAE International Winter Meeting. Paper No. 92-2521.

- Strelkoff, T.S., Clemmens, A.J. 1993. Dimensional analysis in surface irrigation. Manuscript.
- Strelkoff, T.S. 1994. Incorporating management design into surface irrigation simulation. ASAE 1994 International Summer Meeting, Kansas City, Missouri, June 19-22, 1994.
- Talsma, T. 1969. Infiltration from semi-circular furrows in the field. Australian Journal of Soil Research, 1969, No. 7, pages 277-284.
- Tarboton, K.C., Wallender, W.W.I 1989. Field-wide furrow infiltration variability. Trans. ASAE, Vol. 32, No. 3, pages 913-918.
- Trout, T. Unpublished. Installation and use of Powlun v furrow flumes. USDA-Agricultural Research Service, Kimberly, Idaho.
- Trout, T. 1985. Electronic clocks for timing irrigation advance. J. of Irrigation and Drainage Engineering, Vol. 111, No. 1, pages 94-98.
- Trout, T., Mackey, B. 1988a. Inflow-outflow infiltration measurement accuracy. J. of Irrigation and Drainage, Vol. 114, No. 2, 1988, p. 256.
- Trout, T., Mackey, B. 1988b. Furrow flow measurement accuracy. J. of Irrigation and Drainage, Vol. 114, No. 2, 1988, p. 244.
- Trout, T., Mackey, B. 1988c. Furrow inflow and infiltration variability. Trans. ASAE, Vol. 31, No. 2., 1988, p. 531.
- Trout, T. 1990. Surface seal influence on surge flow furrow infiltration. Trans. ASAE, Vol. 35, No. 5, pages 1583-1589.
- Trout, T. 1991. Furrow geometric parameters. J. of Irrigation and Drainage, Vol. 117, No. 5, p. 613.
- Trout, T. 1992a. Furrow flow velocity effect on hydraulic roughness. J. of Irrigation and Drainage, Vol. 118, No. 6, 1992, p. 981.
- Trout, T. 1992b. Flow velocity and wetted perimeter effects on furrow infiltration. Trans. ASAE, Vol. 35, No. 3, p. 855.
- Trout, T.J., Neibling, W.H. 1993. Erosion and sedimentation processes on irrigated fields. J. of Irrigation and Drainage Engineering, Vol. 119, No. 6, pages 947-963.

- Trout, T.J., Sojka, R.E., Lentz, R.D. 1993. Polyacrylamide effect on furrow erosion and infiltration. Paper presented at the 1993 International Summer Meeting, Spokane, WA. Paper No. 93-2036.
- Tunio, A.F. 1994. Sediment loss of furrow irrigation in Malheur County, Oregon. M.S. Thesis, Oregon State University, Corvallis.
- Undersander, D.J., Regier, C. 1988. Effect of tillage and furrow irrigation timing on efficiency of preplant irrigation. *Irrigation Science*, Vol. 9, 1988, p. 57.
- Vogel, T., Hopmans, J.W. 1992. Two-dimensional analysis of furrow infiltration. *Journal of Irrigation and Drainage Engineering*, Vol. 118, No. 5, pages 791-806.
- Walker, W.R., Humpherys, A.S., 1983. Kinematic-wave furrow irrigation model. *J. of Irrigation and Drainage Engineering*, Vol. 109, No. 4, pages 377-392.
- Walker, W.R., Willardson, L.S. 1983. Infiltration measurements for simulating furrow irrigation. *Advances in Infiltration*. ASAE Proceedings of the National Conference on Advances in Infiltration, December 12-13, 1983, Chicago, Illinois, p. 241-248.
- Walker, W.R., Busman, J.D. 1990. Real-time estimation of furrow infiltration. *Journal of Irrigation and Drainage Engineering*, Vol. 116, No. 3, pages 299-318.
- Wilke, O., Smerdon, E.T. 1965. A solution to the irrigation advance problem. *Journal of Irrigation and Drainage*, ASCE, Vol. 91, No. 3, p. 23-24.

APPENDICES

Appendix A Field descriptions

Field B7 at the O.S.U. Malheur Experiment Station:

Field length:	192 m	640 feet	
Crop:	Spring wheat		1993
	Winter wheat		1994
Furrow spacing:	0.76 m	30 in	1993
	0.76 m	30 in	1994
Irrigated spacing:	1.52 m	60 in	1993
	1.52 m	60 in	1994
Field slope:	10 to 60 ft		0.0075 m m ⁻¹
	60 to 100		0.0064
	110 to 160		0.0044
	160 to 210		0.0053
	210 to 260		0.0058
	260 to 310		0.0052
	310 to 360		0.0050
	360 to 410		0.0046
	410 to 460		0.0033
	460 to 510		0.0044
	510 to 560		0.0045
560 to 610		0.0044	
Soil type:	Owyhee and Greenleaf silt loams		
Water source:	Owyhee Ditch and/or well		
Hardware:	Gated pipe with valves, weed screen.		

Field B3 at the O.S.U. Malheur Experiment Station:

Field length:	76.2 m	250 feet	
Crop:	Spring wheat		1993
	Potatoes		1994
Furrow spacing:	0.76 m	30 in	1993
	0.91 m	36 in	1994
Irrigated spacing:	1.52 m	60 in	1993
	1.83 m	72 in	1994
Field slope:	0 to 50 ft		0.0235 m m ⁻¹
	50 to 100		0.0280
	100 to 150		0.0312
	150 to 200		0.0354
	200 to 250		0.0261
Soil type:	Nyssa silt loam		
Water source:	Owyhee Ditch		

Hardware: Gated pipe with valves, weed screen.

Cruickshank corn field on Oregon Slope:

Field length:	390 m	1280 feet	
Crop:	Field corn		1993
Furrow spacing:	0.76 m	30 in	1993
Irrigated spacing:	1.52 m	60 in	1993
Field slope:	0.006 m m ⁻¹		
Soil type:	Owyhee and Nyssa silt loams		
Water source:	Owyhee Ditch		

Hardware: Earth ditch and siphon tubes, bubbler, weed screen.

Duyn sugar beet field near East Island Road

Field length:	274 m	900 feet	
Crop:	Sugar beets		1993
Furrow spacing:	0.56 m	22 in	1993
Irrigated spacing:	1.12 m	44 in	1993

Field slope:	0 to 100 ft	0.0143 m m ⁻¹
	100 to 200	0.0089
	200 to 300	0.0074
	300 to 400	0.0074
	400 to 500	0.0060
	500 to 600	0.0069
	600 to 700	0.0069
	700 to 800	0.0088
	800 to 900	0.0123

Soil type: Feltham loamy fine sand
 Water source: Unknown

Hardware: Concrete ditch and siphon tubes.

Barlow sugar beet field near Mitchell Butte:

Field length:	378 m	1240 feet	
Crop:	Sugar beets		1994
Furrow spacing:	0.56 m	22 in	1994
Irrigated spacing:	1.12 m	44 in	1994

Field slope:	0 to 100 ft	0.0099 m m ⁻¹
	100 to 200	0.0095
	200 to 300	0.0167
	300 to 400	0.0125

Soil type: Nyssa silt loam
 Water source: Owyhee Ditch, high-line.

Hardware: Concrete ditch and siphon tubes.

Bel-Air Farms winter wheat field:

Field length:	378 m	1240 feet	
Crop:	Winter wheat		1994
Furrow spacing:	0.76 m	30 in	1994
Irrigated spacing:	0.76 m	30 in	1994
Field slope:	0 to 200 ft	0.0072 m m ⁻¹	
	200 to 400	0.0077	
	400 to 600	0.0087	
	600 to 800	0.0117	
	800 to 1000	0.0143	
	1000 to 1200	0.0124	
Soil type:	Nyssa silt loam		
Water source:	Owyhee Ditch, high-line.		

Hardware: Concrete ditch and siphon tubes.

Barlow winter wheat field near Mitchell Butte:

Field length:	378 m	1280 feet	
Crop:	Winter wheat		1994
Furrow spacing:	0.76 m	30 in	1994
Irrigated spacing:	1.52 m	60 in	1994
Field slope:	0 to 50 ft	0.0248 m m ⁻¹	
	50 to 100	0.0238	
	100 to 150	0.0276	
	150 to 200	0.0298	
Soil type:	Nyssa silt loam		
Water source:	Owyhee Ditch, high-line.		

Hardware: Concrete ditch and siphon tubes.

Appendix B Irrigation descriptions

MES Field B7

May 11, 1993. First irrigation of the season. Irrigation began at 3:00 pm and ended at 5:00 pm the following day. Alternating furrows were irrigated. This included both wheel traffic and non-wheel traffic furrows. High temperature for the day was near 90 degrees Fahrenheit. Neutron probe readings were taken on May 11 and May 13. Crop evapotranspiration between neutron probe measurement times was estimated to be 1.67 cm (0.66 inches) using Agrimet data. Inflow rates averaged 0.40 l s^{-1} (6.3 gpm).

June 14, 1993. Second irrigation of the season. First irrigation of these furrows due to alternating furrow strategy. Irrigation began at 9:00 am and ended at 1:30 pm the following day. Neutron probe readings were taken on June 13 and June 18. Crop evapotranspiration between neutron probe measurement times was estimated to be 2.74 cm (1.08 inches) based on Agrimet data. Inflow rates averaged 0.36 l s^{-1} (5.8 gpm).

July 1, 1993. Third irrigation of the season. Second irrigation of these furrows. Irrigation began at 9:00 am and ended at 9:00 am the following day. Neutron probe readings were deemed unreliable because counts were consistently abnormally high. Inflow rates averaged 0.33 l s^{-1} (5.4 gpm).

July 14, 1993. Fourth irrigation of the season. Second irrigation of these furrows. Irrigation began at 10:30 am and ended at 10:30 am the following day. Neutron probe soil moisture readings were deemed unreliable because counts were consistently abnormally high. Inflow rates averaged 0.37 l s^{-1} (5.9 gpm).

July 28, 1993. Fifth irrigation of the season. Third irrigation of these furrows. Irrigation began at 10:00 am and ended at 10:30 am the following day. Neutron probe soil moisture data are incomplete for this irrigation due to instrument failure. Inflow rates averaged 0.37 l s^{-1} (5.9 gpm).

April 5, 1994. First irrigation of winter wheat. Though wheel traffic furrows were irrigated (every other furrow was wheel traffic compacted), intake rates were extremely high, suggesting that wheel traffic effects from the previous fall were no longer important. Inflow rates were purposely varied for the observation furrows, ranging from 0.31 to 0.44 l s^{-1} (5.0 to 7.0 gpm respectively). Inflow-outflow data were obtained for the top 56 m (150 feet) of the field. After 48 hours of irrigation, streams had not yet completely advanced the length of the field and so the irrigation was stopped.

April 26, 1994. Second irrigation of winter wheat following compaction and cultivation. The same furrows were irrigated as those on April 5. Inflow-outflow data were obtained for the top 91 m (300 feet) of the field. A complete irrigation evaluation was not conducted on this date due to the tremendous dissimilarities between the top and bottom of the field following the first irrigation. Inflow rates similarly ranged from 0.31 to 0.44 l s^{-1} (5.0 to 7.0 gpm) for this irrigation. Soil moisture was high in the top half of the field prior at the time of cultivation.

Bel-Air Farms

April 12, 1994. First irrigation of winter wheat following a rotation in alfalfa. Every furrow was irrigated which included both wheel and non-wheel furrows. The irrigation start was at 9:00 am and the irrigation ended at 10:00 am the following morning. The average flow rate was 0.51 l s^{-1} (8.1 gpm).

MES Field B3

June 1, 1994. First irrigation of potatoes. All furrows irrigated on this date are wheel traffic furrows. Alternating furrows were irrigated. A randomized block design was used to implement straw mulched experimental plots. Both strawed and non-strawed furrows were irrigated. Irrigation began at 2:00 pm and ended at 2:00 pm the following day. The average inflow rate was 0.17 l s^{-1} (2.8 gpm). Neutron probe soil moisture data was collected on May 31 and June 3, 1994. Crop evapotranspiration between neutron probe measurement times was estimated to be 0.96 cm (0.38 inches) based on Agrimet data.

June 9, 1994. Second irrigation of the season. All non-wheel traffic furrows were irrigated for this irrigation. Both strawed and non-strawed furrows were irrigated. Irrigation started at 9:00 am and ended at 7:30 am the following day. The average inflow rate was approximately 0.18 l s^{-1} (2.9 gpm). Neutron probe readings were taken on June 8 and June 11, 1994. Crop evapotranspiration between the neutron probe measurements was estimated to be 1.47 cm (0.58 inches).

June 15, 1994. Third irrigation of the season. All wheel traffic furrows were irrigated. Both strawed and non-strawed furrows were irrigated. The irrigation started at 11:50 am and ended at 12:00 am (midnight) for the straw mulched furrows and 12:00 pm the following day for the non-strawed furrows. The average inflow rate for this irrigation was 0.18 l s^{-1} (2.9 gpm). June 14 and June 17 were the dates of the neutron probe soil moisture measurements. Evapotranspiration between the neutron probe measurement times was estimated to be 1.88 cm (0.74 inches) based on Agrimet data for these dates.

June 22, 1994. Fourth irrigation of the season. All non-wheel traffic furrows were irrigated. Both strawed and non-strawed furrows were irrigated. Irrigation started at 2:00 pm and ended at 2:00 pm two days later (set time of 48 hours). The average inflow rate was 0.21 l s^{-1} (3.3 gpm). June 22 and 26 were the dates of the neutron probe measurements and crop evapotranspiration was estimated to be 3.66 cm (1.44 inches) between these dates based on Agrimet data.

Duyn Sugar beets

September 3, 1993. A late season irrigation of Sugar beets. Both wheel and non-wheel traffic furrows were irrigated (every other furrow was a wheel traffic furrow). The irrigation started at 7:20 am and ended at approximately 7:30 am the following morning. Average inflow rate was 0.62 l s^{-1} (9.85 gpm). In non-wheel traffic furrows, the irrigation stream advanced rapidly, only slightly slower than wheel traffic furrows. Towards late morning, the stream in the non-wheel traffic furrows began receding due to an apparent increase in the furrow intake rate. After nightfall, the irrigation streams completed their advance. The weather was sunny and warm with a high in the mid 80's

Cruickshank corn

July 22, 1993. Irrigation of corn following cultivation. Crop height was approximately 1.5 m (5 feet). Weather was cool and cloudy with a high temperature in the mid 70's (Fahrenheit). Inflow rates averaged 0.52 l s^{-1} (8.3 gpm). Irrigation start time was 9:00 am and irrigation ended at 9:45 am on the following day.

Barlow Sugar beets

April 11, 1994. First irrigation of Sugar beets prior to emergence. Irrigation water was treated with polyacrylamide (PAM) to reduce erosion and improve intake. The exact rate of PAM application is unknown but it was somewhat in excess of 1.1 kg ha^{-1} (1 lb ac^{-1}) based on the entire surface area of the field. Advance and inflow-outflow data were obtained for the first 91.4 (300 ft) of furrow. A full irrigation evaluation was not conducted. The mean inflow rate for the observed furrows was 0.15 l s^{-1} (2.4 gpm).

Barlow winter wheat

May 10, 1994. Second irrigation of this winter wheat field. First irrigation for these furrows based on an alternating furrow irrigation strategy. Advance and inflow-outflow data were recorded for the first 61 m (200 ft). A complete irrigation evaluation was not conducted. The mean flow rate for the observation furrows was 0.35 l s^{-1} (5.5 gpm).

Appendix C Variable notation

a	Exponent to the Extended Kostiakov equation (dim)
a	Coefficient to the SCS intake equation ($L \cdot T^{-b}$)
A	Irrigation adequacy (%)
A	Cross-sectional flow area (L^2)
A_o	Cross-sectional flow area at top of field (L^2)
AE	Application efficiency (%)
AW	Available water (L)
AWC	Available water capacity ($L \cdot L^{-1}$)
b	Coefficient to the Extended Kostiakov equation ($L^3 L^{-1} T^{-1}$), approximates the long term intake rate
b	Exponent to the SCS intake equation (dim)
b	Furrow channel bottom width (L)
c	Constant to the Extended Kostiakov equation ($L^3 L^{-1}$)
C	Chezy's C for hydraulic roughness ($L^{1/2} T^{-1}$)
D_{rz}	Effective depth of root zone (L)
DU	Distribution uniformity (dim)
ϵ_{DI}	Error in average infiltrated depth (%)
ϵ_h	Error in measurement of upstream head(L)
ϵ_Q	Error in flow measurement (%)
fc	Field capacity (%)
F	Channel section factor ($L^{8/3}$)
Fr	Froude number (dim)
g	Acceleration due to gravity ($L \cdot T^{-2}$)
h	Upstream head (L)
h	Soil-water potential (L)
h_t	Soil-water tension (L)
h_g	Soil-water gravitational potential (L)
k	Coefficient to the Extended Kostiakov intake equation ($L^3 L^{-1} T^{-a}$)
$K(h)$	Hydraulic conductivity as a function soil-water potential ($L \cdot T^{-1}$)
L	Field length (L)
MAD	Management allowed depletion (%)
n	Manning's roughness coefficient ($T \cdot L^{1/3}$)
n	Number of field observations
θ_c	Critical soil moisture content ($L \cdot L^{-1}$)
θ_i	Initial soil moisture content ($L \cdot L^{-1}$)
θ_v	Volumetric soil moisture content ($L \cdot L^{-1}$)
p	Coefficient to power advance equation ($L \cdot T^{-r}$)
pwp	Permanent wilting point volumetric soil moisture content (%)
P	Wetted perimeter (L)
P_n	Theoretical wetted perimeter calculated from normal depth (L)

q	Darcy flux ($L \cdot T^{-1}$)
Q	Flowrate ($L \cdot T^{-1}$)
Q_o	Furrow inflow rate ($L \cdot T^{-1}$)
Q_{avg}	Mean furrow flow rate ($L^3 T^{-1}$)
Q_{ro}	Furrow runoff flow rate ($L^3 T^{-1}$)
r	Exponent to power advance curve (dim)
R	Hydraulic radius (L)
RAW	Readily available water (L)
s	Distance (L)
S_f	Friction slope ($L \cdot L^{-1}$)
S_o	Field slope ($L \cdot L^{-1}$)
t	Elapsed time (T)
t_i	Time of completion of advance (T)
t_{ro}	Time of end of runoff (T)
τ	Intake opportunity time (T)
T	Stream top-width (L)
$T_m(x_i)$	Advance time from field observation at point x_i (T)
$T_s(x_i)$	Advance time from simulation at point x_i (T)
$V_{applied}$	Volume of water applied (L^3)
V_{bu}	Volume of water beneficially used (L^3)
V_{obs}	Observed volume (L^3)
V_{pred}	Predicted volume (L^3)
V_t	Total runoff volume (L^3)
V^*	Normalized runoff volume (dim)
W	Irrigated furrow spacing (L)
y	Flow depth (L)
y_c	Critical flow depth (L)
y_n	Normal flow depth (L)
Z	Cumulative intake ($L^3 L^{-1}$)
Z_{avg}	Average infiltrated depth (L)
Z_{lq}	Average lower quarter depth of infiltration (L)
Z_N	Normalized cumulative intake ($L^3 L^{-2}$)
Z_{req}	Required depth of irrigation (L)

Appendix D Infiltration tests

Table A.1 Recirculating infiltrometer test results from MES Field B7 conducted during 1993. The field was planted to spring wheat. Soil type was a Greenleaf silt loam.

Date	Furrow type	Initial soil moisture		Total intake after 10 hrs l m ⁻¹
		30 cm cm cm ⁻¹	60 cm cm cm ⁻¹	
July 2	Non-wheel	0.13	0.18	161
July 27	Non-wheel	0.22	0.23	155
August 13	Wheel	0.14	0.16	123
August 28	Non-wheel	0.14	0.16	119
Sept. 8	Wheel	0.23	0.22	108

Table A.2 Inflow-outflow infiltration test results from MES Field B7 conducted during 1994. The field was planted to winter wheat. Soil type was a Greenleaf silt loam.

Date	Furrow type	Initial soil moisture		Total intake after 10 hrs l m ⁻¹
		30 cm cm cm ⁻¹	60 cm cm cm ⁻¹	
April 5	Wheel*	0.21	0.24	218
April 5	Wheel*	0.21	0.24	283
April 5	Wheel*	0.21	0.24	248
April 26	Wheel	0.22	0.24	56
April 26	Wheel	0.22	0.24	38

* Wheel traffic effects no longer important at time of irrigation.

Table A.3 Inflow-outflow infiltration test results from MES Field B3 conducted during 1993. The field was planted to potato. Soil type was a Nyssa silt loam.

Date	Furrow type	Initial soil moisture		Total intake after 10 hrs l m ⁻¹
		30 cm cm cm ⁻¹	60 cm cm cm ⁻¹	
June 1	Wheel	0.21	0.24	31
June 1	Wheel	0.21	0.24	20
June 1	Wheel, straw	0.21	0.24	33
June 1	Wheel, straw	0.21	0.24	45
June 9	Non-wheel	0.22	0.26	94
June 9	Non-wheel	0.22	0.26	38
June 9	Non-wheel, straw	0.22	0.26	150
June 15	Wheel	0.23	0.28	20
June 15	Wheel	0.23	0.28	16
June 15	Wheel, straw	0.23	0.28	38
June 15	Wheel, straw	0.23	0.28	41

Table A.4 Inflow-outflow infiltration test results from 1994 from three farm sites. Soils were all Nyssa silt loam.

Date	Farm, furrow type	Initial soil moisture		Total intake after 10 hrs l m ⁻¹
		30 cm cm cm ⁻¹	60 cm cm cm ⁻¹	
April 11*	Barlow, wheel	na	na	30
April 11*	Barlow, wheel	na	na	49
April 12	Bel-Air, non-wh.	0.21	0.29	109
April 12	Bel-Air, wheel	0.21	0.29	82
May 10**	Barlow, non-wh.	0.11	0.16	80
May 10**	Barlow, wheel	0.11	0.16	49

* Barlow sugar beet field.
**Barlow winter wheat field.

Table A.5 Summary of SFR simulation results

Field ID	Date	Irrig. Eff. %	Adeq. %	Dist. Unif. %	Inflow Vol. m ³	Inflow Depth cm	Runoff Vol. m ³	Runoff Depth cm	D. Perc. Vol. m ³	D. Perc. Depth cm
MES B7 W	5/11/93	65.63	0.00	90.80	37.10	12.71	12.21	4.18	0.00	0.00
MES B7 NW	5/11/93	70.75	74.44	49.40	37.44	12.83	0.14	0.05	10.86	3.72
MES B7 W	6/14/93	52.02	100.00	84.60	34.18	11.71	7.81	2.68	8.46	2.90
MES B7 NW	6/14/93	50.60	100.00	67.90	35.14	12.04	2.48	0.85	14.77	5.06
Duyn W	9/03/93	50.77	84.19	72.30	52.71	17.18	17.24	5.62	8.75	2.85
Duyn NW	9/03/93	47.22	88.88	55.70	57.46	18.72	1.33	0.43	29.06	9.47
Bel-Air W	4/12/94	37.22	100.00	64.90	44.82	16.11	5.27	1.89	22.70	8.16
Bel-Air NW	4/12/94	50.23	52.74	1.20	46.81	16.83	0.00	0.00	23.20	8.34
Cruickshank	7/22/93	82.66	59.73	68.60	46.57	7.86	2.32	0.39	5.81	0.98
MES B3 W ST	6/01/94	27.50	0.00	92.30	14.18	10.17	10.25	7.35	0.00	0.00
MES B3 W NST	6/01/94	18.80	0.00	94.30	15.04	10.79	12.21	8.76	0.00	0.00
MES B3 NW ST	6/09/94	58.75	87.59	61.60	15.15	10.86	0.73	0.52	5.48	3.93
MES B3 NW NS	6/09/94	60.46	84.49	84.90	14.91	10.69	4.37	3.13	1.52	1.09

Appendix F Field observations

Table A.6 Field observed irrigation performance

Field Description	Date	Time hrs	Furrow type	Length m	Inflow lps	Slope %	Sp. m	Soil m cm/cm	Drz cm	Zreq cm	Inflow m ³	Runoff m ³
B7 MES	5/11/93	26	W	195	0.40	0.55	1.52	0.27	120	10	37.10	12.90
B7 MES	5/11/93	26	NW	195	0.40	0.55	1.52	0.27	120	10	37.50	0.00
B7 MES	6/14/93	28	W	195	0.35	0.55	1.52	0.30	120	6	34.10	9.00
B7 MES	6/14/93	28	NW	195	0.36	0.55	1.52	0.30	120	6	35.00	4.30
B7 MES	7/01/93	24	W	195	0.33	0.55	1.52	0.29	120	7	28.10	5.80
B7 MES	7/01/93	24	NW	195	0.32	0.55	1.52	0.29	120	7	28.20	1.50
B7 MES	7/14/93	24	W	195	0.36	0.55	1.52	0.30	120	6	32.00	14.60
B7 MES	7/14/93	24	NW	195	0.37	0.55	1.52	0.30	120	6	32.50	7.80
B7 MES	7/29/93	24	W	195	0.36	0.55	1.52	0.30	120	6	31.20	11.00
B7 MES	7/29/93	24	NW	195	0.37	0.55	1.52	0.30	120	6	31.60	6.00
B Cruickshank	7/22/93	24.75	NW	390	0.52	0.60	1.52	0.24	61	7	45.01	2.44
B Cruickshank	7/22/93	24.75	NW	390	0.54	0.60	1.52	0.24	61	7	44.76	2.05

Table A.6

Field Description	Date	Time hrs	Furrow type	Length m	Inflow lps	Slope %	Sp. m	Soil m cm/cm	Drz cm	Zreq cm	Inflow m ³	Runoff m ³
R. Saito	7/07/93	12		155.5	0.11	0.56	1.02	0.22	61	8	4.39	0.00
R. Saito	7/07/93	12		155.5	0.16	0.56	1.02	0.22	61	8	6.52	0.00
R. Saito	7/07/93	12		155.5	0.14	0.56	1.02	0.22	61	8	5.66	0.00
R. Saito	7/07/93	12		155.5	0.14	0.56	1.02	0.22	61	8	5.44	0.00
B. Duyn	8/03/93	24	W	274	0.62	0.88	1.12	0.15	105	9	52.70	17.10
B. Duyn	8/03/93	24	NW	274	0.67	0.88	1.12	0.15	105	9	57.50	0.60
B. Duyn	8/03/93	24	W	274	0.55	0.88	1.12	0.15	105	9	47.30	16.90
B. Duyn	8/03/93	24	NW	274	0.66	0.88	1.12	0.15	105	9	55.70	0.10
Bel-Air	4/12/94	24	W	366	0.52	1.03	0.76	0.30	120	6	46.30	13.20
Bel-Air	4/12/94	24	NW	366	0.52	1.03	0.76	0.30	120	6	46.80	0.00
Bel-Air	4/12/94	24	W	366	0.50	1.03	0.76	0.30	120	6	44.80	5.75
B3 MES	6/01/94	24	W	76.2	0.18	3.02	1.83	0.23	61	8	15.80	12.49
B3 MES	6/01/94	24	W, ST	76.2	0.18	3.02	1.83	0.23	61	8	15.10	10.46
B3 MES	6/01/94	24	W, ST	76.2	0.17	3.02	1.83	0.23	61	8	14.20	10.04
B3 MES	6/01/94	24	W	76.2	0.17	3.02	1.83	0.23	61	8	15.00	12.09

Table A.6

Field Description Date Time Furrow Length Inflow Slope Sp. Soil m Drz Zreq Inflow Runoff
 hrs type m lps % m cm/cm cm cm m³ m³

B3 MES	6/09/94	22.5	NW	76.2	0.18	3.02	1.83	0.24	61	6.5	14.80	4.37
B3 MES	6/09/94	22.5	NW, S	76.2	0.19	3.02	1.83	0.24	61	6.5	15.10	0.90
B3 MES	6/09/94	22.5	NW, S	76.2	0.19	3.02	1.83	0.24	61	6.5	15.30	0.00
B3 MES	6/09/94	22.5	NW	76.2	0.17	3.02	1.83	0.24	61	6.5	13.70	9.49
B3 MES	6/15/94	24	W	76.2	0.18	3.02	1.83	0.26	61	5.5	15.29	12.84
B3 MES	6/15/94	12.5	W, ST	76.2	0.18	3.02	1.83	0.26	61	5.5	8.18	5.18
B3 MES	6/15/94	12.5	W, ST	76.2	0.18	3.02	1.83	0.26	61	5.5	8.00	4.99
B3 MES	6/15/94	24	W	76.2	0.17	3.02	1.83	0.26	61	5.5	14.94	13.40
B3 MES	6/22/94	48	NW	76.2	0.19	3.02	1.83	0.24	61	7	33.27	7.72
B3 MES	6/22/94	48	NW, S	76.2	0.15	3.02	1.83	0.24	61	7	26.49	1.06
B3 MES	6/22/94	48	NW, S	76.2	0.21	3.02	1.83	0.24	61	7	36.69	0.00
B3 MES	6/22/94	48	NW	76.2	0.20	3.02	1.83	0.24	61	7	34.34	20.79